SCINTILLATION COUNTERS

- FAST, FLEXIBLE, CHEAP
  - BEAM COUNTERS

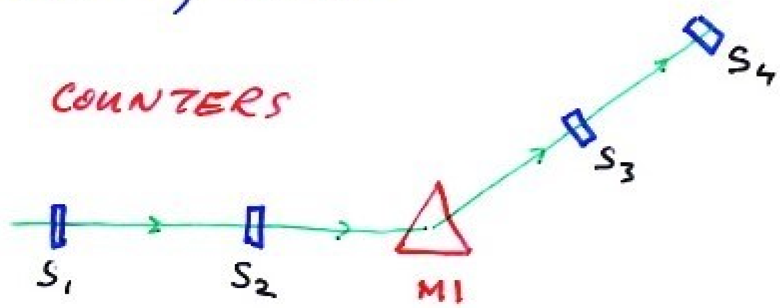

COINCIDENCE $S_1 \cdot S_2 \cdot S_3 \cdot S_4$
DEFINES PARTICLE TRAJECTORY

- TIME OF FLIGHT — PARTICLE ID

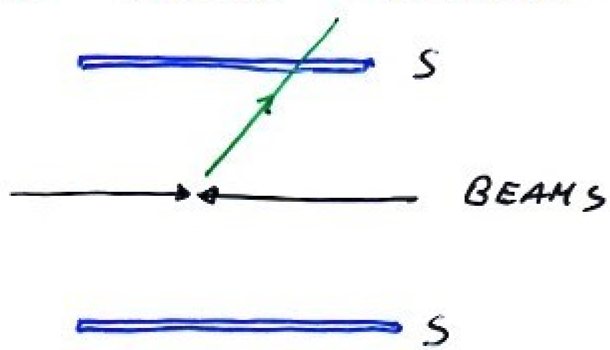

- SAMPLING CALORIMETER

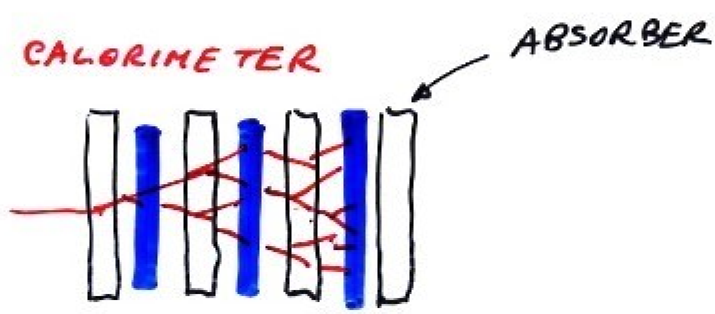

Scintillators

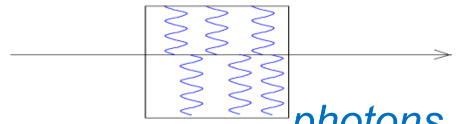

- Charged particle passing through matter distorts
  - atom
  - molecule
  - lattice
- Relaxation of distortion – light emitted

$$p^{\pm} + A \rightarrow p^{\pm} + A^{*}$$
$$A^{*} \rightarrow A + \gamma$$

- Emitted photon may – excite another molecule

Successive excitation & emission – different λ photons

$$p^{\pm} + A \rightarrow p^{\pm} + A^{*}$$
$$A^{*} + B \rightarrow A + B^{*}$$
$$B^{*} + C \rightarrow C^{*} + B$$
$$C^{*} \rightarrow C + \gamma$$

each step $\sim 100\ ps$

whole chain $\sim 1-10\ ns$

- Very fast – good timing resolution

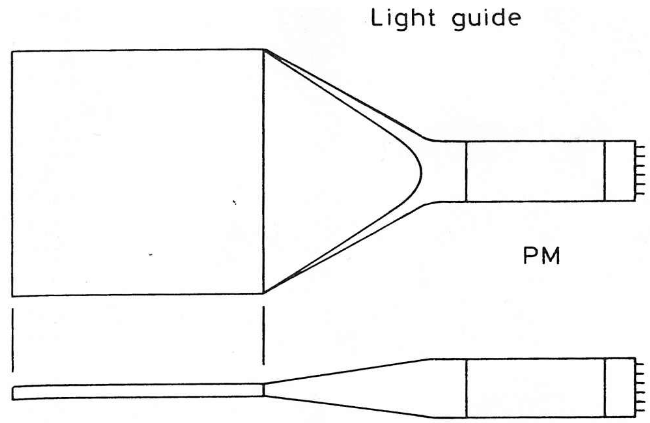

Fig. 9.6. Adapting a flat scintillator sheet to the circular face of a PM with a light guide

- Can be extremely efficient $\frac{dE}{dx} \sim 2\, MeV\,/\,cm$

$$1\gamma\,/\,10^2\,eV\ \text{lost} \rightarrow 10^4\,\gamma\,/\,cm$$

$$\times\ \text{collection efficiency}$$

$$\times\ \text{photomultiplier efficiency}$$

~ 100 photoelectrons per cm.

- Spatial resolution ~ size of scintillator ~10s cm $\sim 10\mu$

Scintillating fibres

TYPICAL SCINTILLATOR

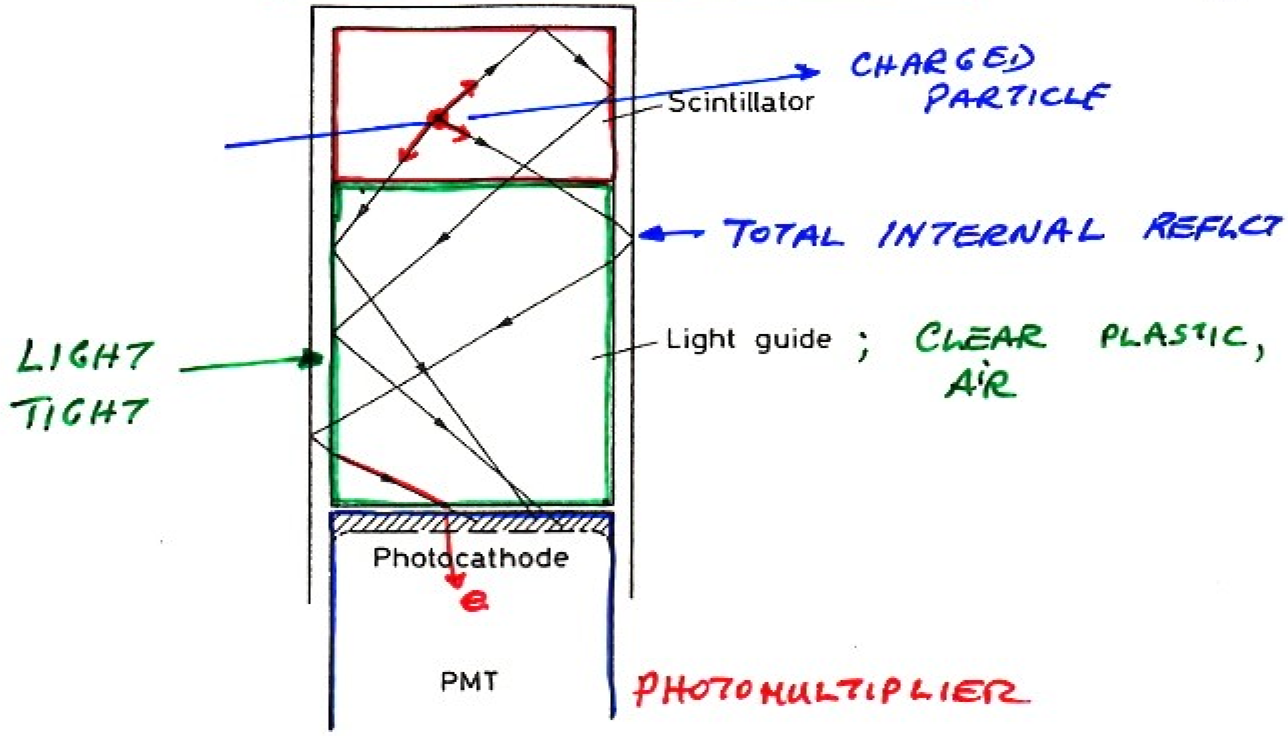

Fig. 9.5. Example of scintillator-PM coupling with a light guide

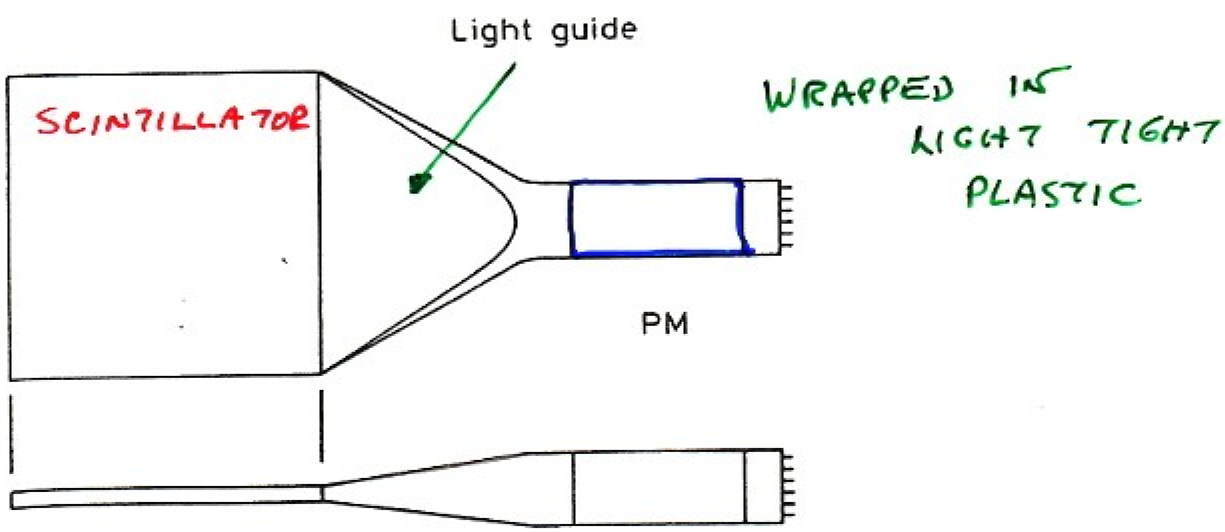

Fig. 9.6. Adapting a flat scintillator sheet to the circular face of a PM with a light guide


56 AVP

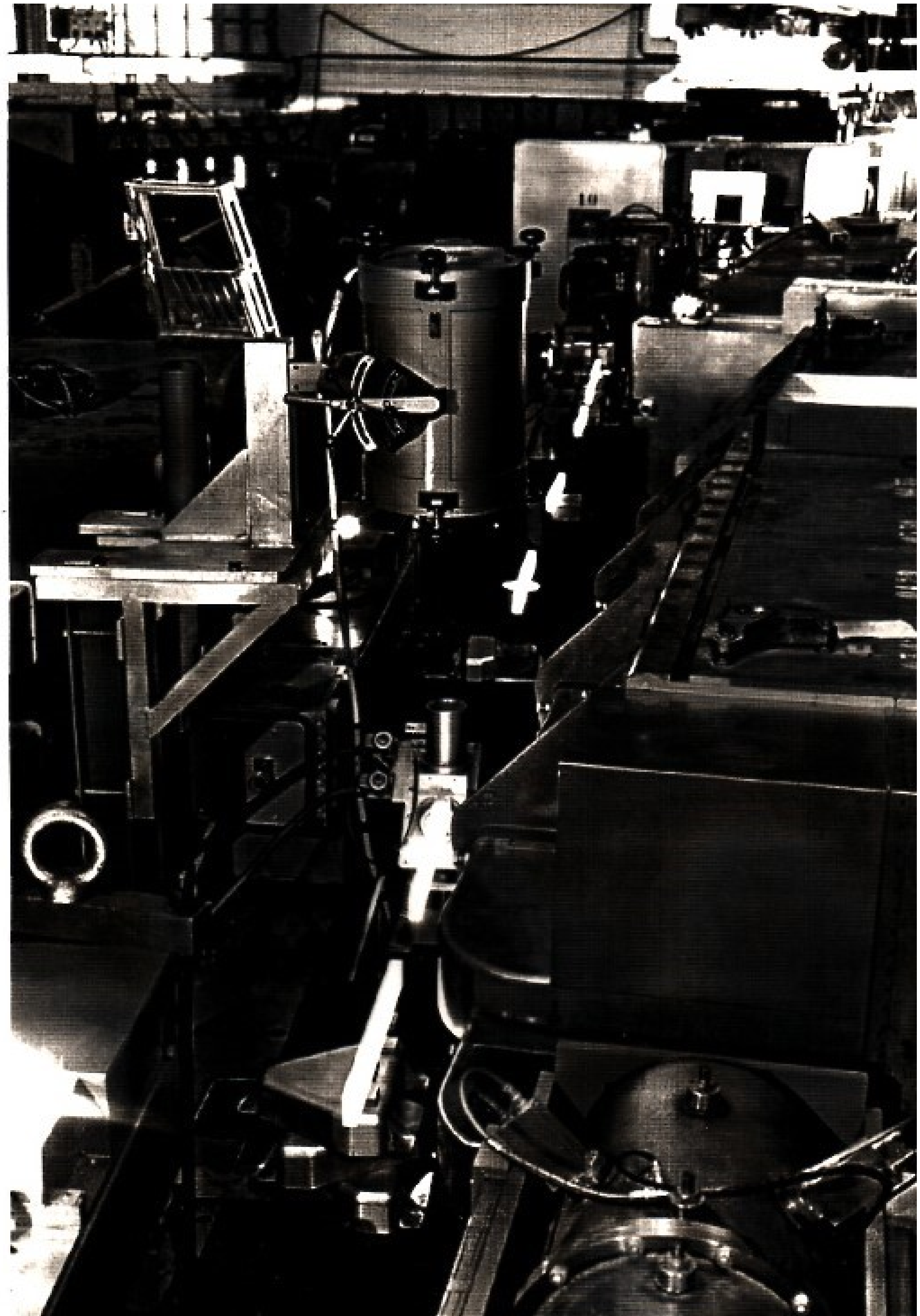

Scintillator Hodoscope

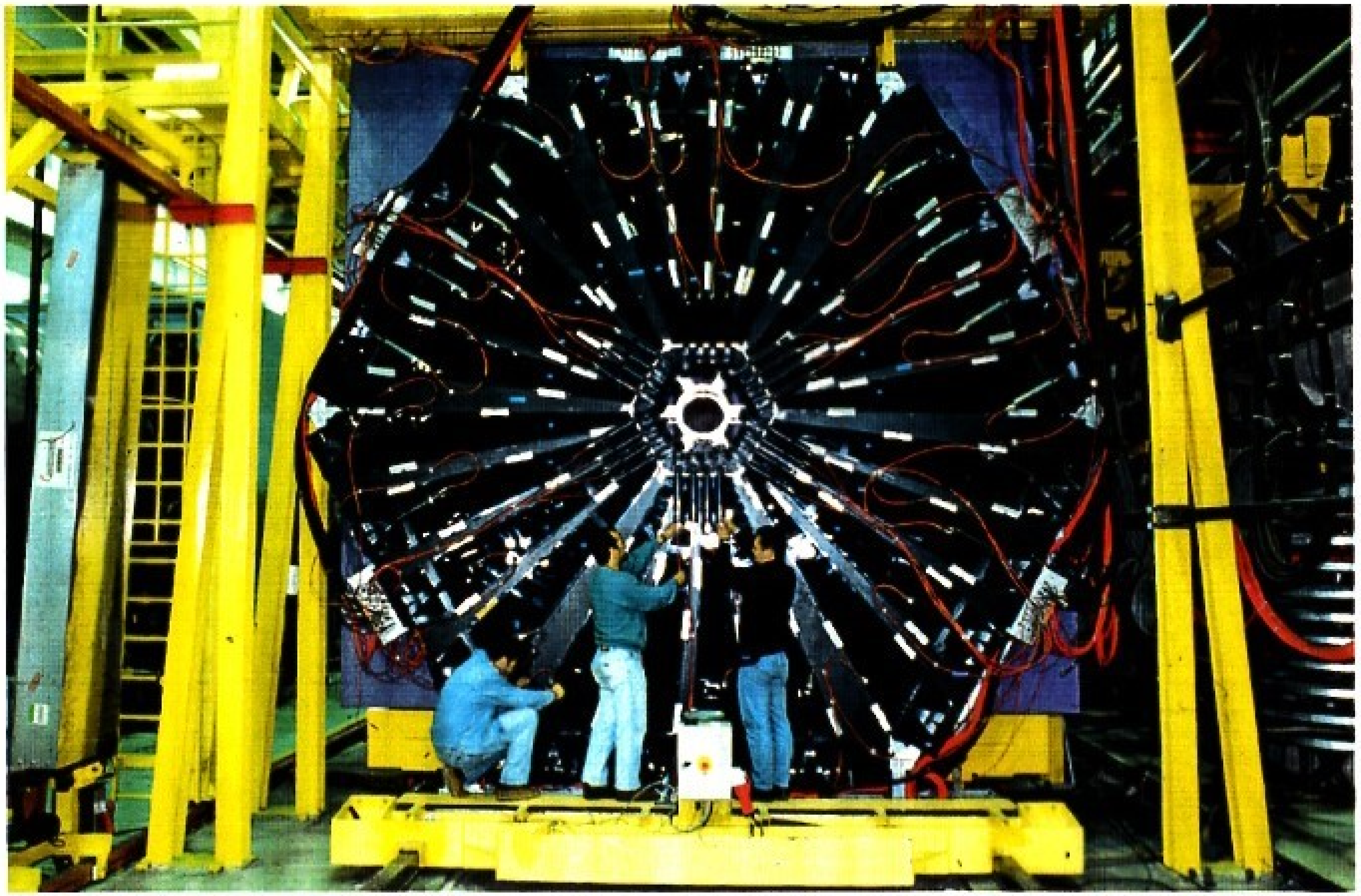

SCINTILLATING MATERIAL

- NOBLE GASES   He Ne Ar Kr

  FAST ~ 1ns
  UV
  LOW DENSITY
  } NOT USUALLY PRACTICAL

- INORGANIC CRYSTALS   NaI, BaF_2, BGO, CsI, $PbWO_4$

  → HIGH RESOLUTION EM CALORIMETER

  HIGH EFFICIENCY   1γ / 25eV
  DENSE $X_0 \sim 1$cm
  ~~FAST~~ SLOW! $\tau \sim 100$ns
  EXPENSIVE

- ORGANIC SCINTILLATORS

  FAST
  CHEAP

  - PLASTICS — FLEXIBLE   POLYSTYRENE LOADED WITH PBD, PPO, POPOP (COMPLEX)

  - LIQUIDS   SOLVENT + (COMPLEX)

    → CHEAP
    ↳ LARGE SCALE
    eg ν CALORIMETERS

ORGANIC SOLIDS & LIQUIDS

They usually consist of a solvent + scintillator and a secondary fluor as wavelength shifters.

A traversing ionizing particle releases energy in the solvent. Then, energy flows radiationless* to the scintillator. Finally, light emitted by the scintillator is absorbed (radiative transfer**) and re-emitted at longer wavelength by the secondary fluor.

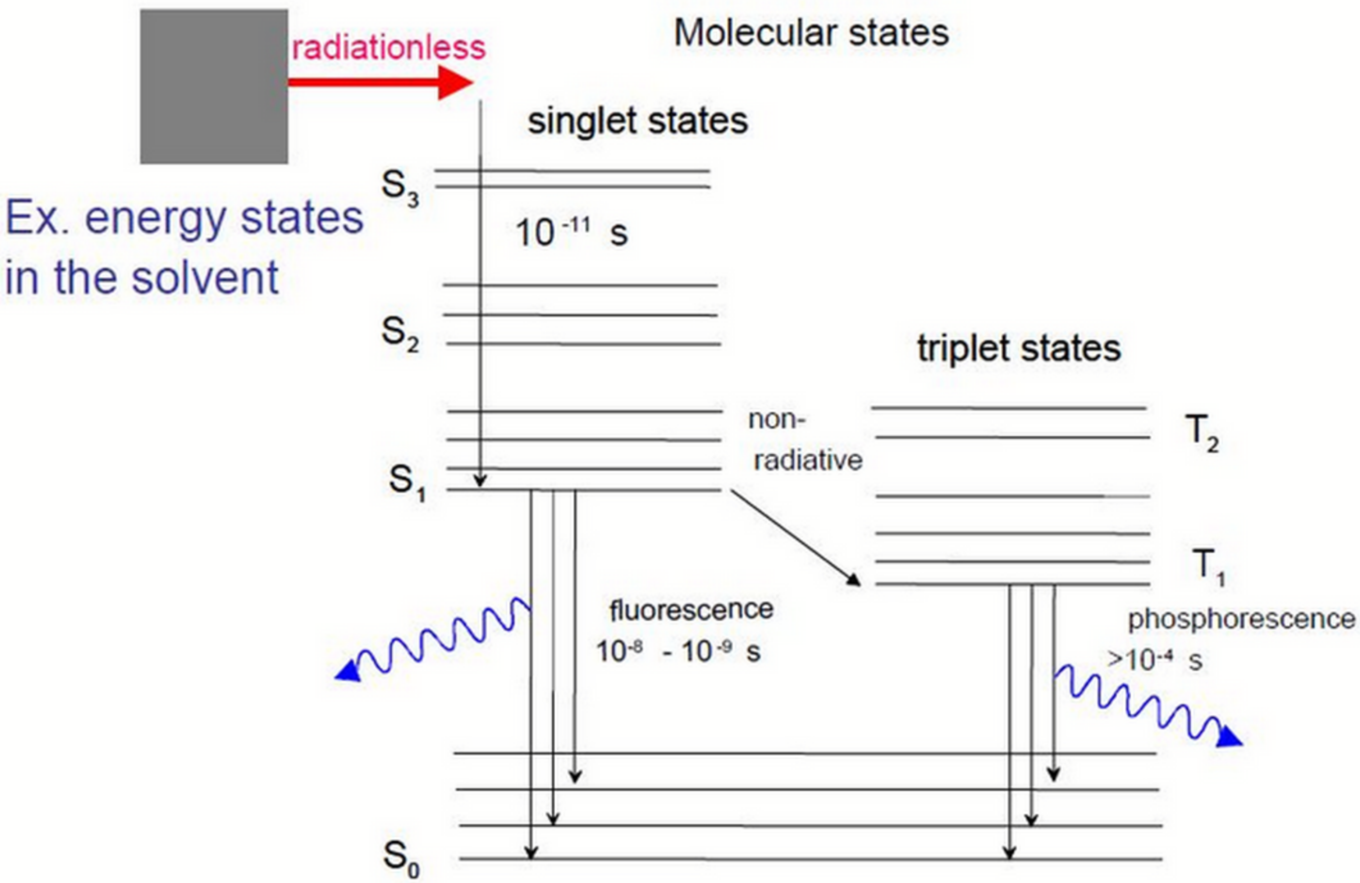

A fluor has its absorption and emission spectra shifted. The two peaks difference is called Stokes shift

*fast and local energy transfer via non-radiative dipole-dipole interactions (Förster transfer).

**~$1/R^2$ light attenuation

Why are scintillators transparent to emitted light?

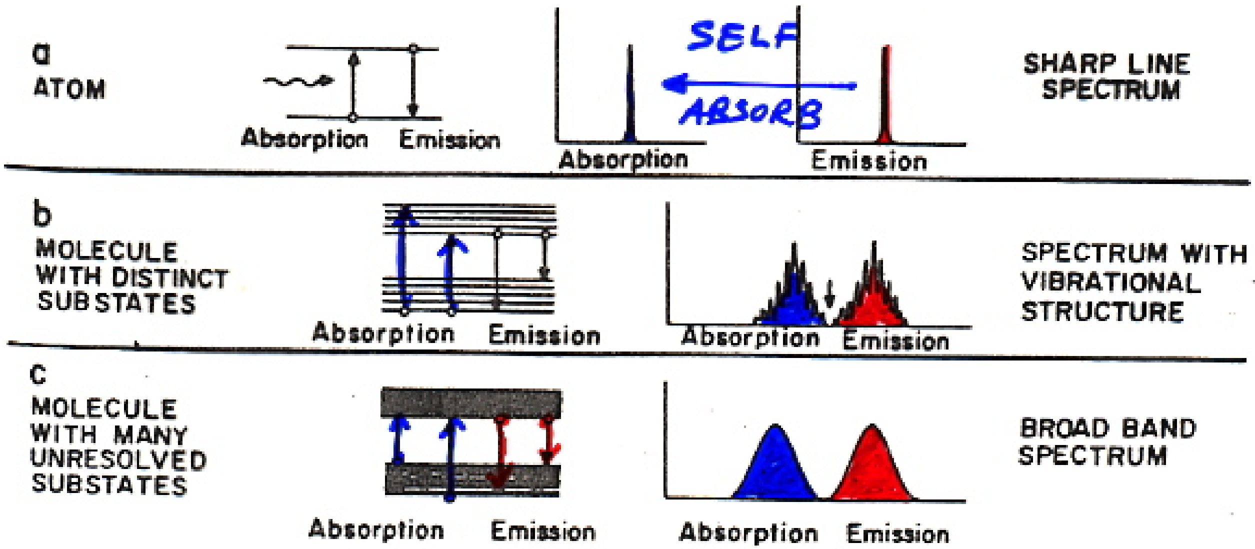

- Stokes shift

• TIME SCALE OF SCINTILLATION

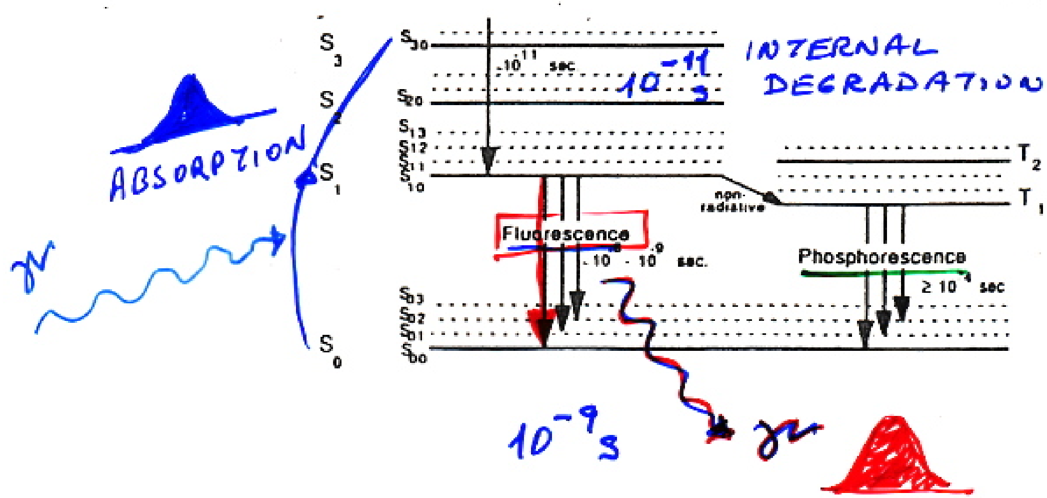

Abs. and emission spectra

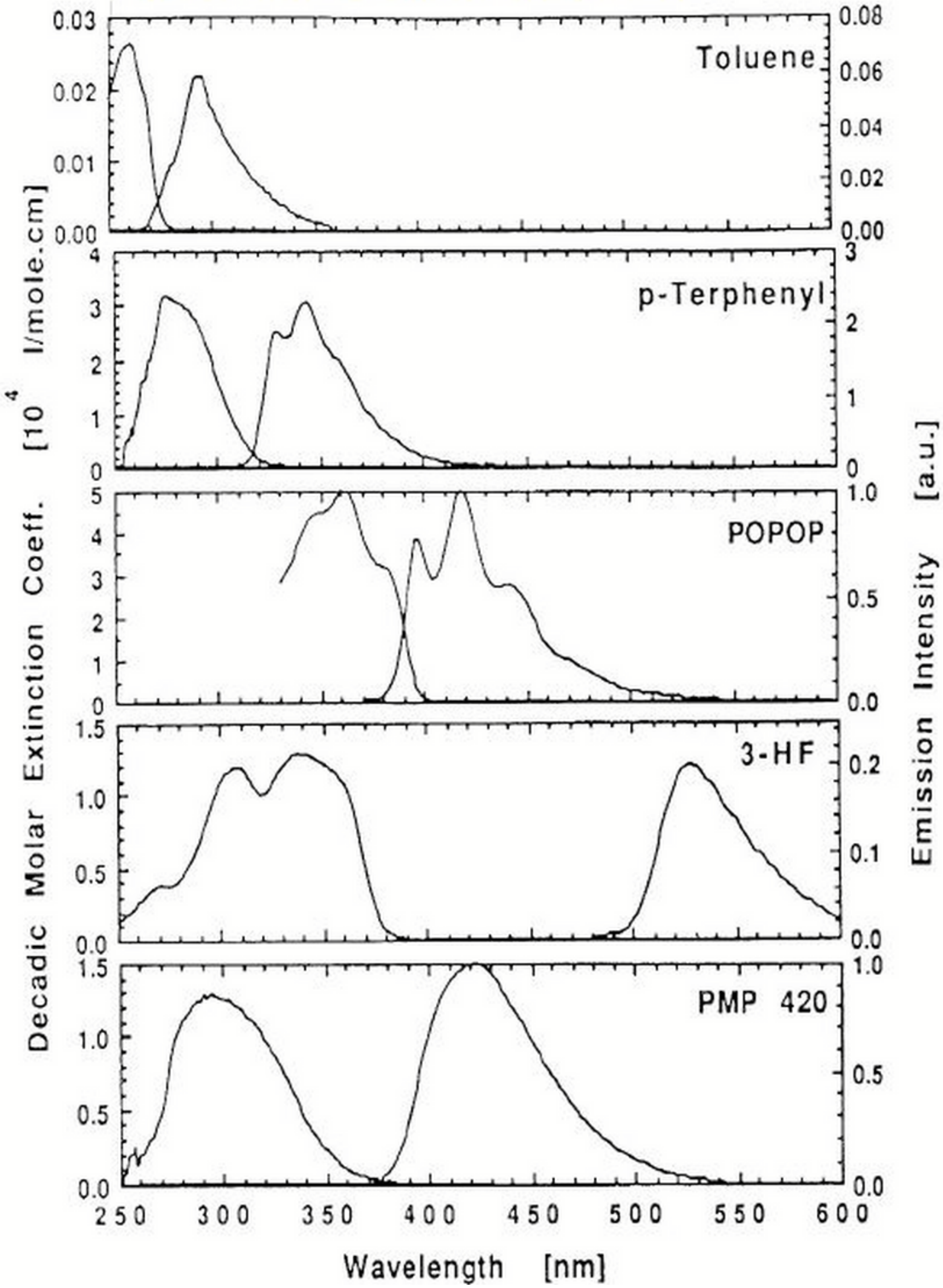

ADD DIFFERENT WAVE SHIFTING PHOSPHORS – TUNE FINAL WAVELENGTH

MATCH SENSITIVITY OF PHOTODETECTOR

RADIATION HARDNESS

Wavelength Shifting

• PRIMARY SCINTILLATION MAY BE UNDETECTABLE → UV

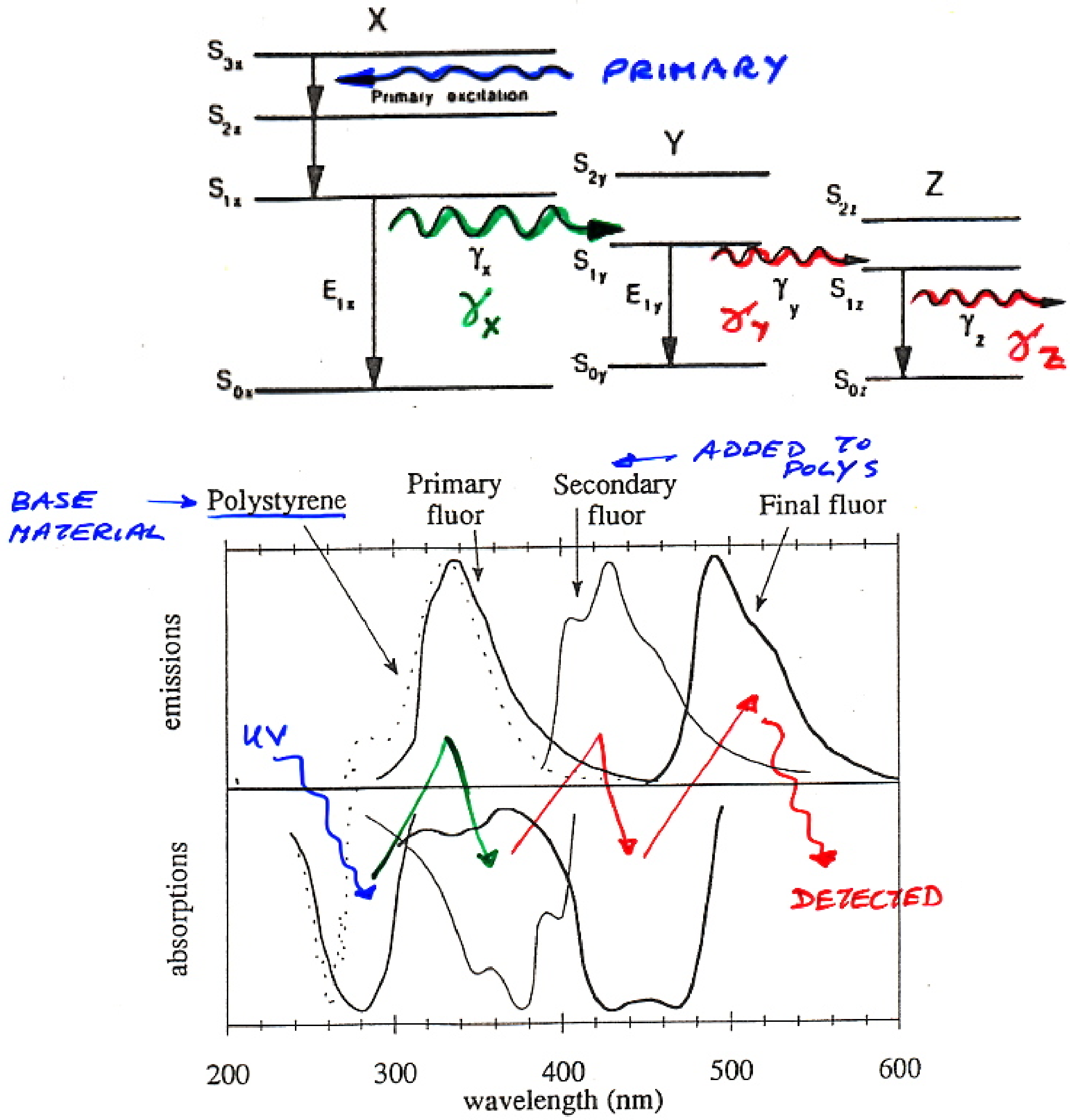

WAVELENGTH SHIFTING

→ GEOMETRY

• ONLY LIGHT TRAPPED BY TOTAL INTERNAL REFLECTION TRAPPED

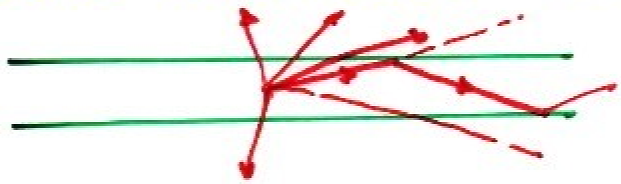

→ LIMITED GEOMETRICAL EFFICIENCY

? HOW TO TURN LIGHT AROUND CORNER ?

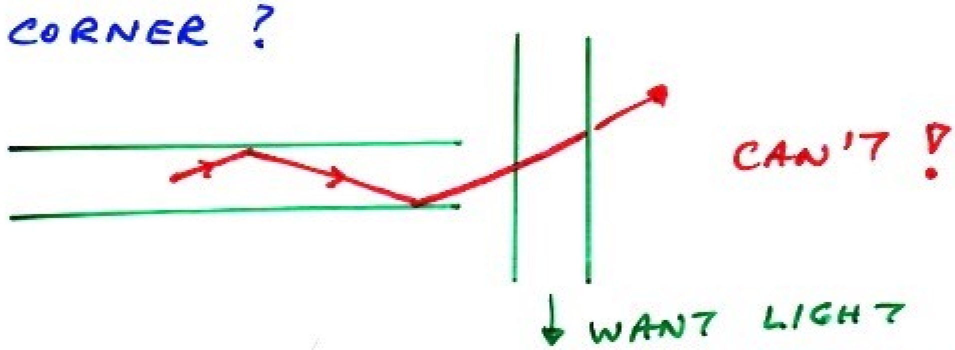

• ABSORB + RE-EMIT

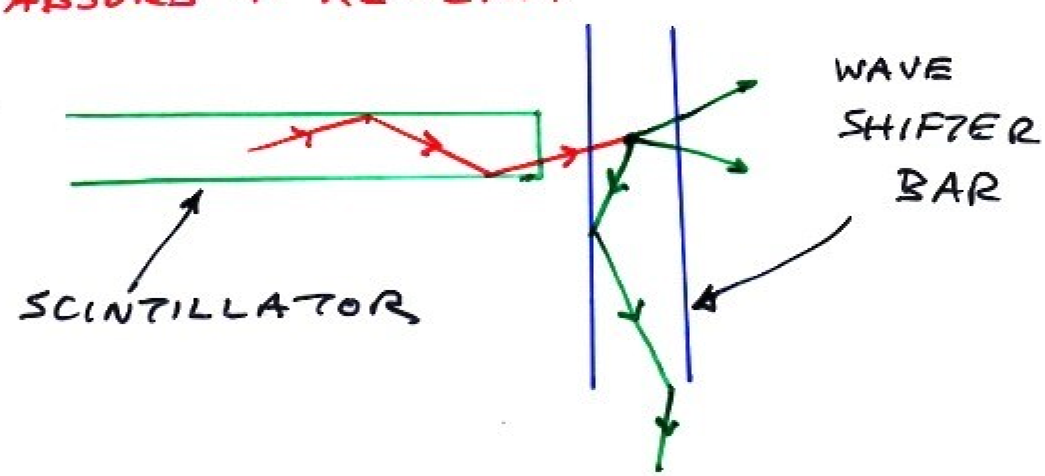

ZEUS CALORIMETER

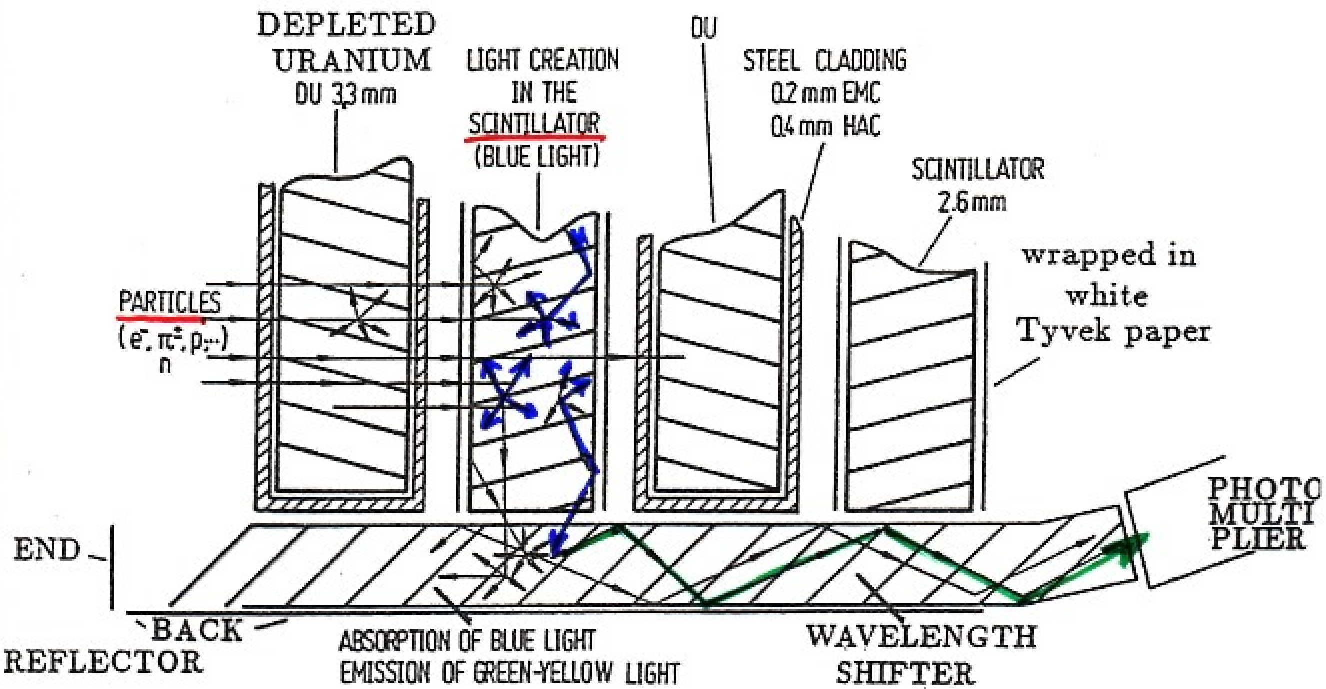

Fig. 2.44 Readout of the scintillator light with wavelength shifters.

- WAVE SHIFTER TECHNIQUE

→ COMPACT, CRACK LESS SCINTILLATING SAMPLING CALORIMETER

INORGANIC CRYSTALS

EM CALORIMETERS

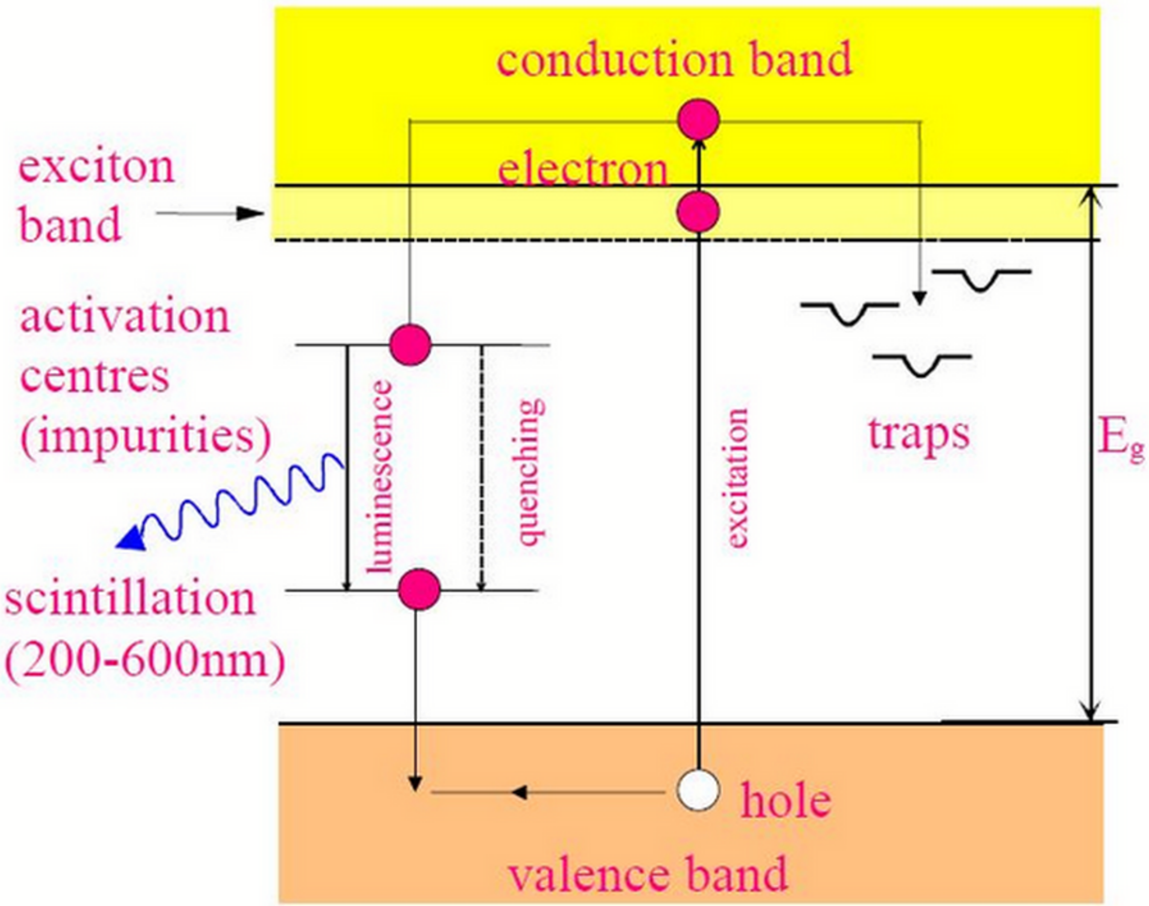

Warning, sometimes ≥ 2 time constants:

- fast recombination (ns-μs) from activation centers
- delayed recombination due to trapping (μs-ms)

•full control of growth, doping and impurities is imperative to optimize light yield, transmission and decay time

Scintillator composition	Density (g/cm^3)	Index of refraction	Wavelength of max.Em. (nm)	Decay time Constant (μs)	Scinti Pulse height[1)]	Notes
NaI(Tl)	3.67	1.9	410	0.25	100	2)
CsI	4.51	1.8	310	0.01	6	3)
CsI(Tl)	4.51	1.8	565	1.0	45	3)
CaF_2(Eu)	3.19	1.4	435	0.9	50	
BaF_2	4.88	1.5	190/220 310	0,0006 0.63	5 15	
BGO	7.13	2.2	480	0.30	10	
$CdW0_4$	7.90	2.3	540	5.0	40	
$PbWO_4$	8.28	2.1	440	0.020	0.1	
CeF_3	6.16	1.7	300 340	0.005 0.020	5	
GSO	6.71	1.9	430	0.060	40	
LSO	7	1.8	420	0.040	75	
YAP	5.50	1.9	370	0.030	70	

1) Relative to NaI(Tl) in %; 2) Hygroscopic; 3) Water soluble

Liquefied noble gases: LAr, LXe, LKr

NEUTRINO EXPTS ✓
DARK MATTER EXPTS

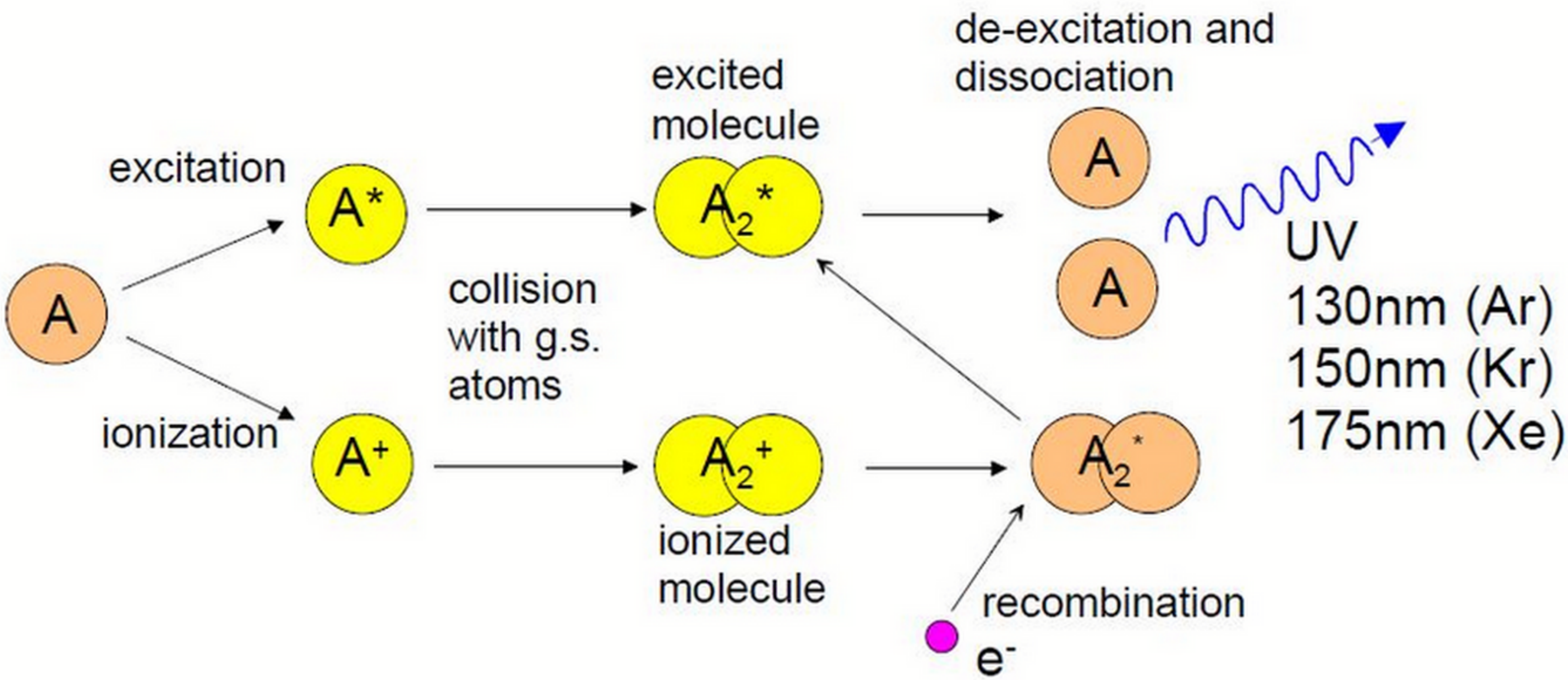

Also here one finds 2 time constants: from a few ns to 1 μs.

SCINTILLATING FIBRES

Large volume liquid or solid detectors (in form of tiles): underground experiments, sampling calorimeters (HCAL in CMS or ATLAS, etc.), counters, light guides.

High precision, small volume active targets and fibre tracking (UA2, D0, CHORUS).

As an example, a scintillating plastic fibre working principle:

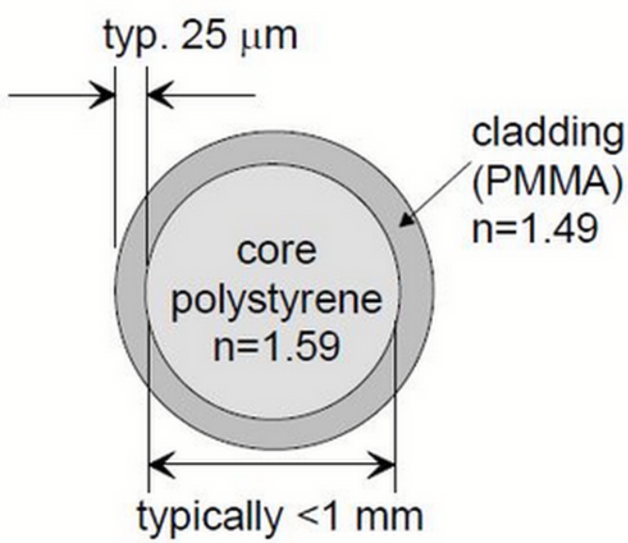

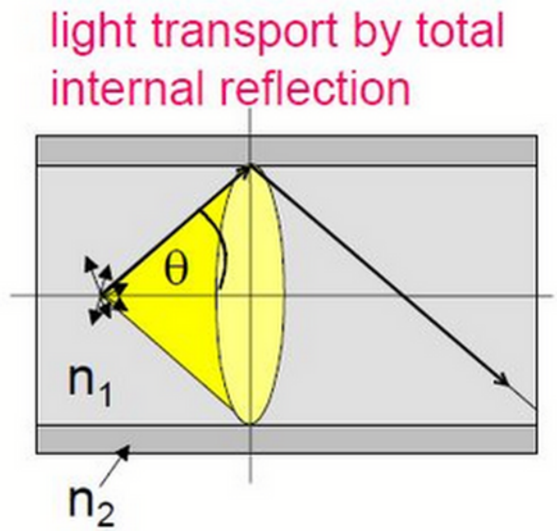

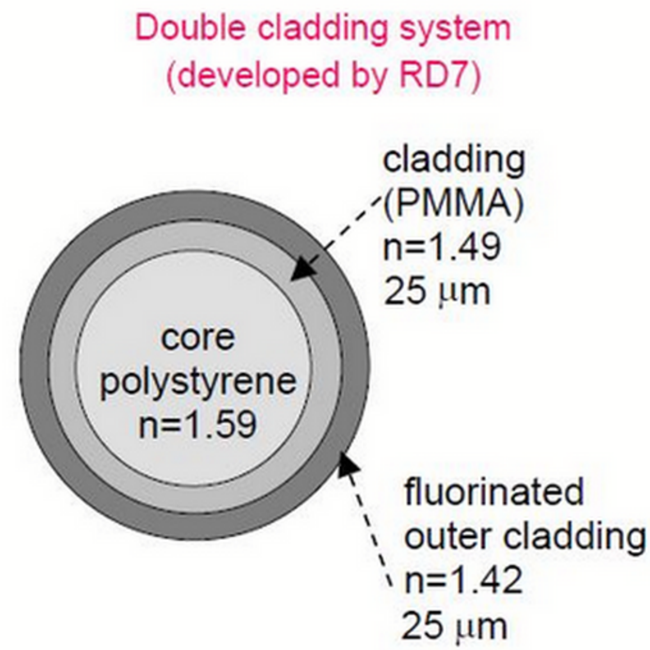

$$\frac{d\Omega}{4\pi} = 0.5\,(1-\cos^2\theta) = 3\%$$

$$\theta \le \arccos\frac{n_2}{n_1} \approx 69.6^\circ$$

$$\frac{d\Omega}{4\pi} = 0.5\,(1-\cos^2\theta) \approx 5.3\%$$

ACTIVE TARGET

ALSO DØ CENTRAL TRACKER

Developed in RD7, they consist of bundles of hexagonal fibres (typ. 60 μm dia., 2.5 mm bundle size)

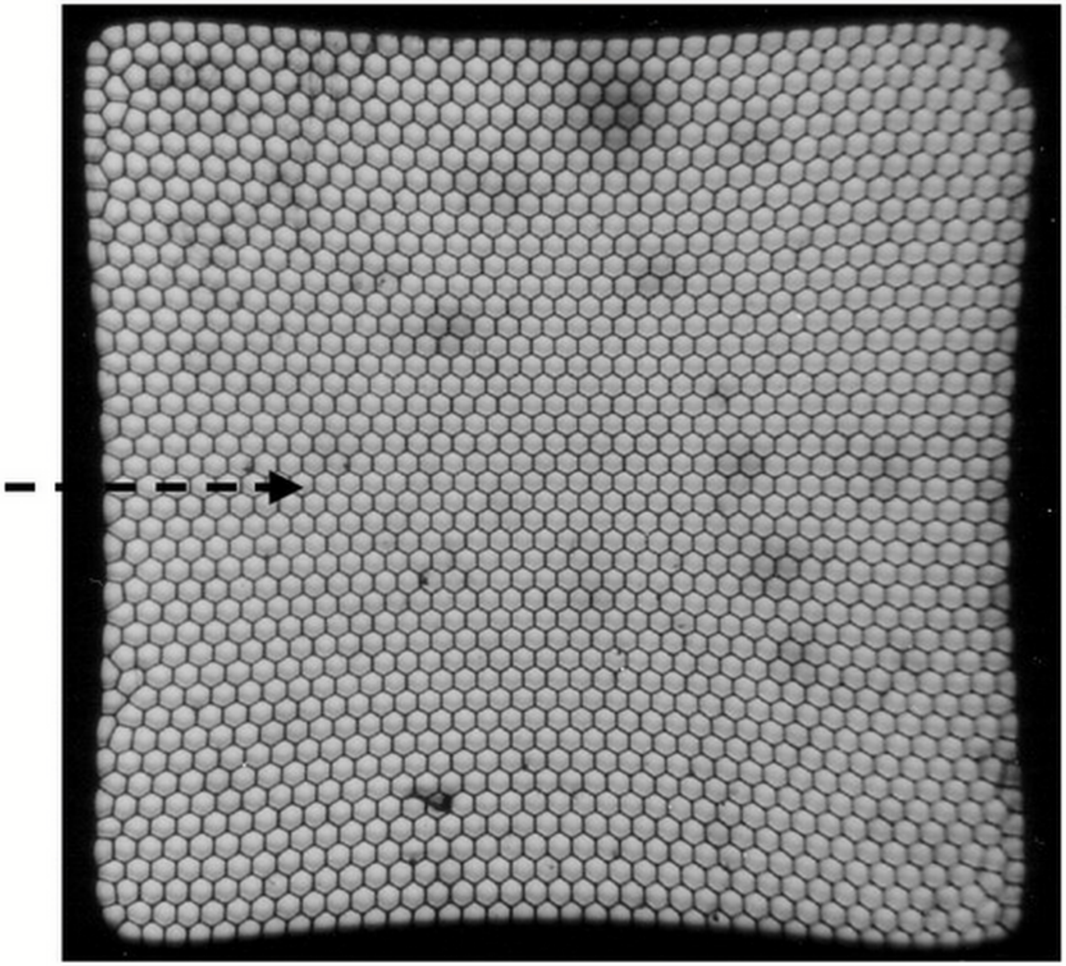

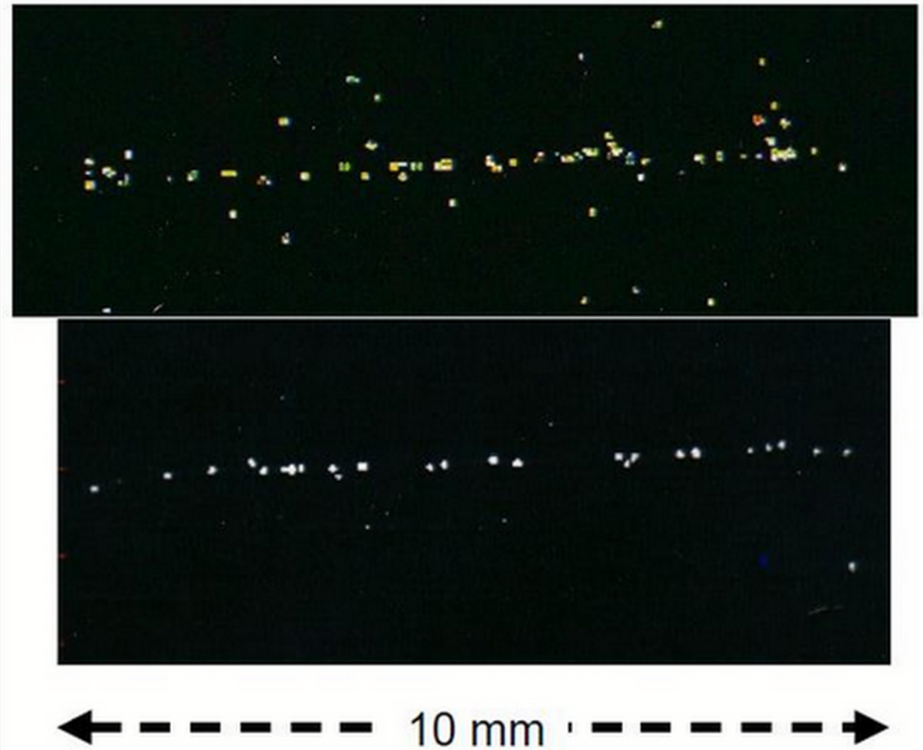

Images of tracks from 5 GeV/c pions (1989)

Beautiful tracks with only **2.2% of X_0 and >20 hits**, but…

READ OUT USING IMAGE INTENSIFIERS

Active target in WA84 (1989)

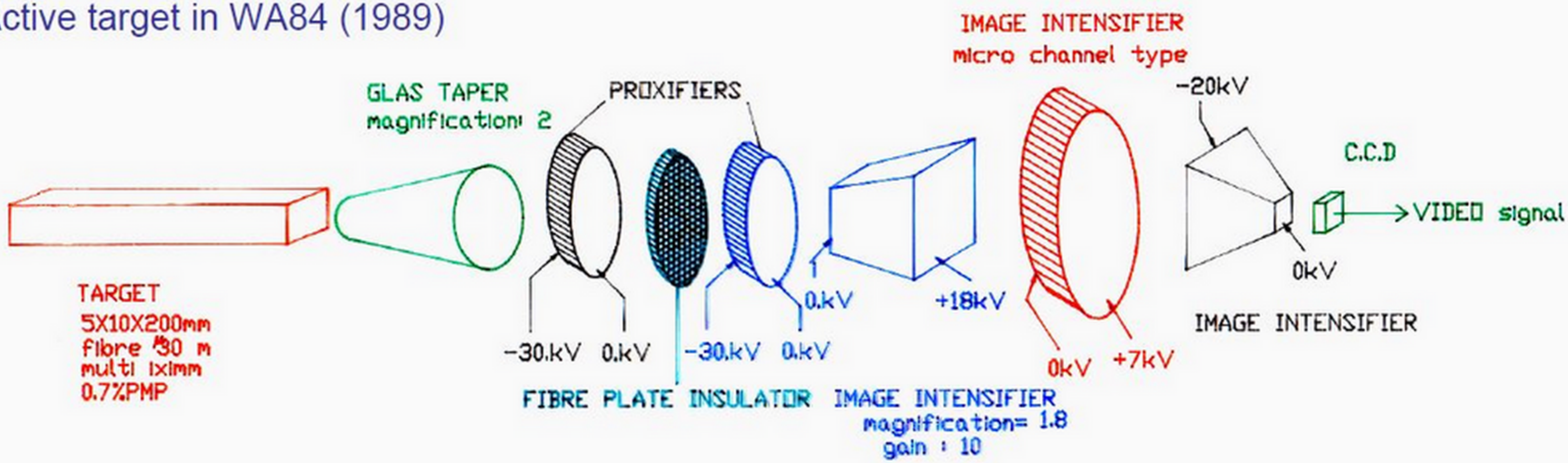

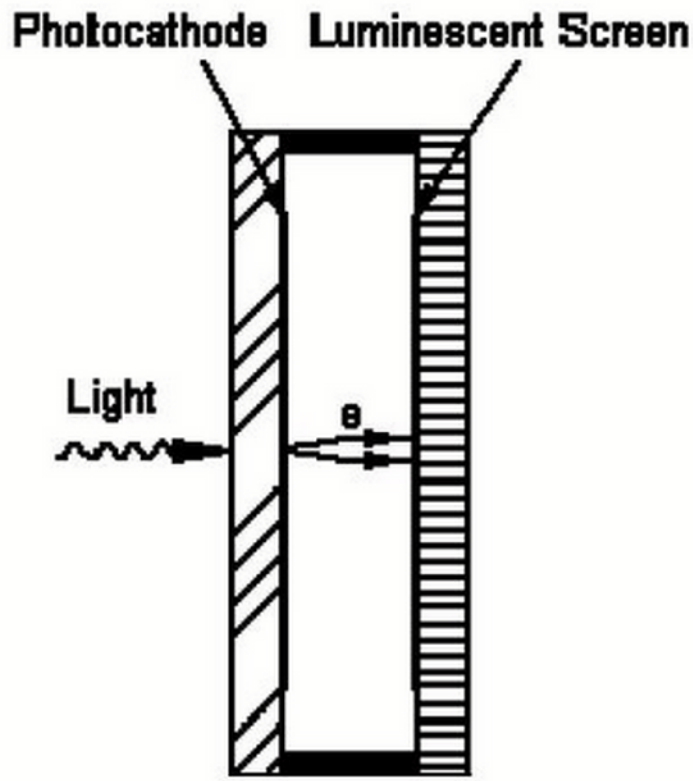

Proximity focus image intensifier PROXIFIER® (1. generation image intensifier)

Light impinges upon the photocathode through the input window of the image intensifier. Due to the photoelectric effect, electrons are produced which escape from the photocathode with very little energy. By a high potential electrical acceleration field between photocathode and phosphor screen of 10 kV to 15 kV, the electrons are strongly accelerated and, at the same time, closely focused. They strike the phosphor screen with high kinetic energy and stimulate fluorescence.

The fluorescent screen is covered on its upper side, which is turned facing the photocathode, with two layers:

Scintillating tile readout via fibers and photomultipliers

ATLAS TILECAL

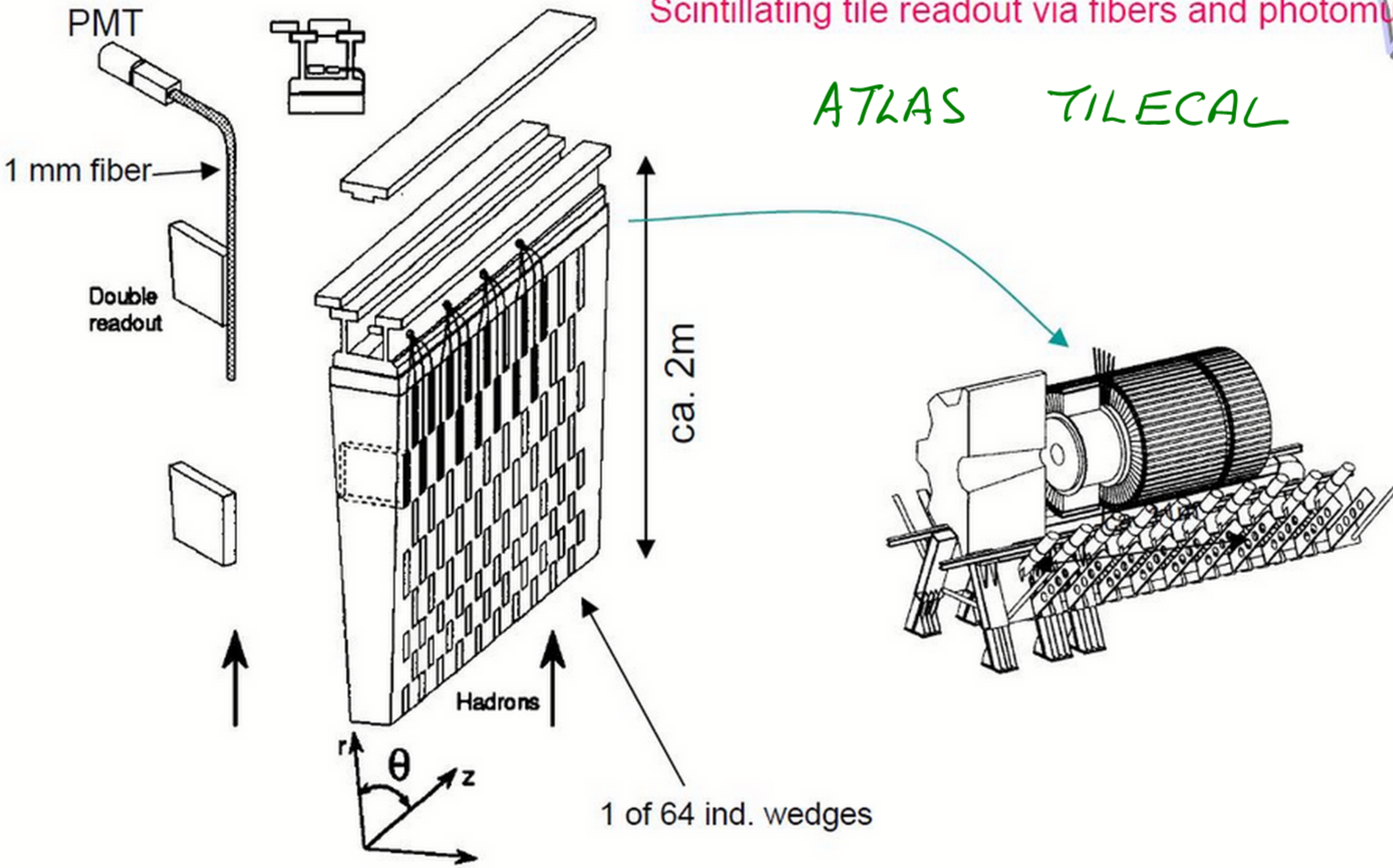

Periodical arrangement of scintillator tiles (3 mm thick) in a steel absorber structure

(ATLAS TDR)

Photomultiplier

$$\text{Gain} = (\text{secondary emission factor } \delta)^N$$

$\delta = kV_d$

number of stages

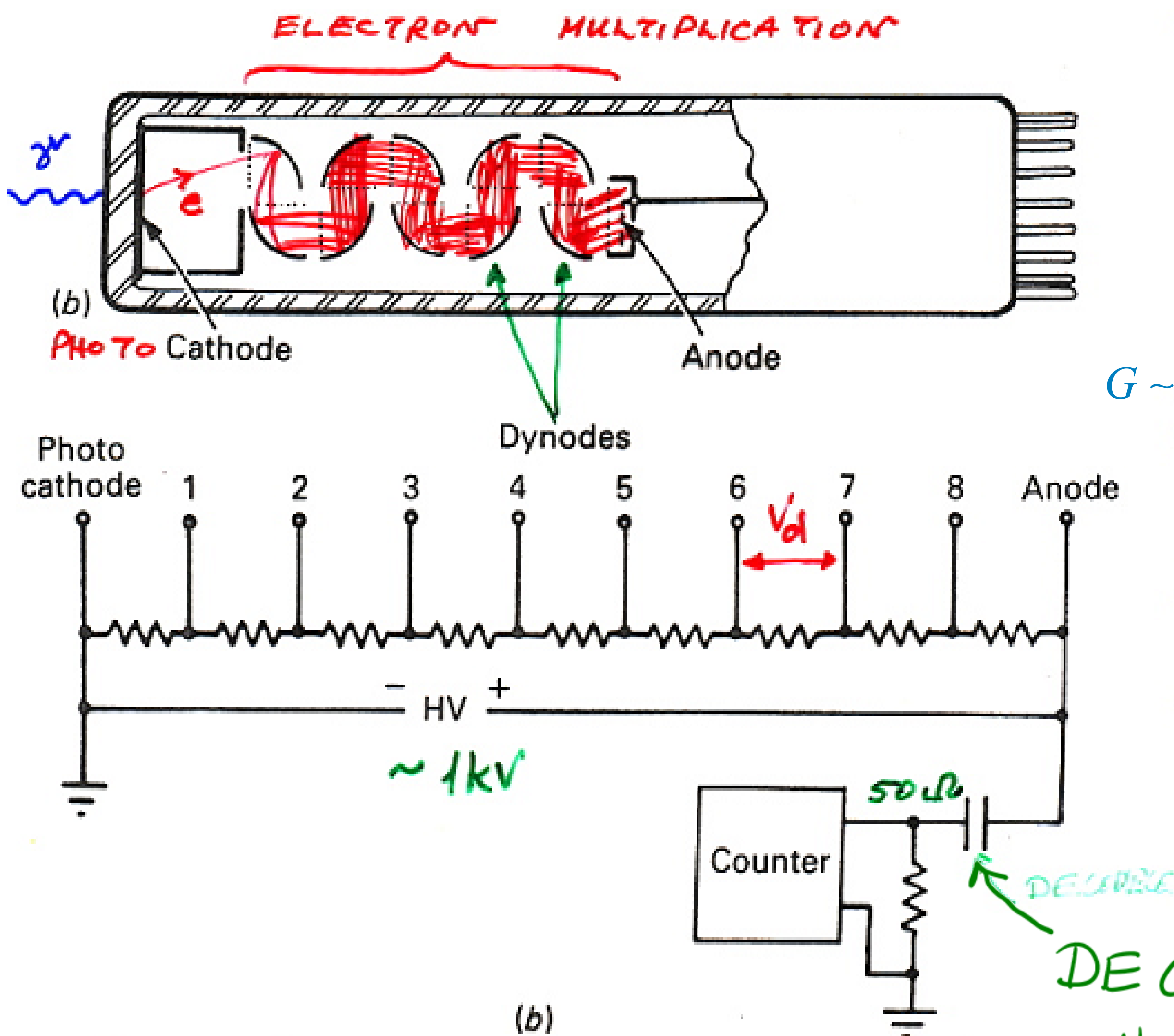

$G \sim 10^7$

$$\frac{1 \text{ electron x } 10^7}{10ns} \rightarrow 1mA$$

$50\Omega = 50mV$

DECOUPLE HIGH VOLTAGE

- Fast
- Low noise
- High gain

PM Sensitivity

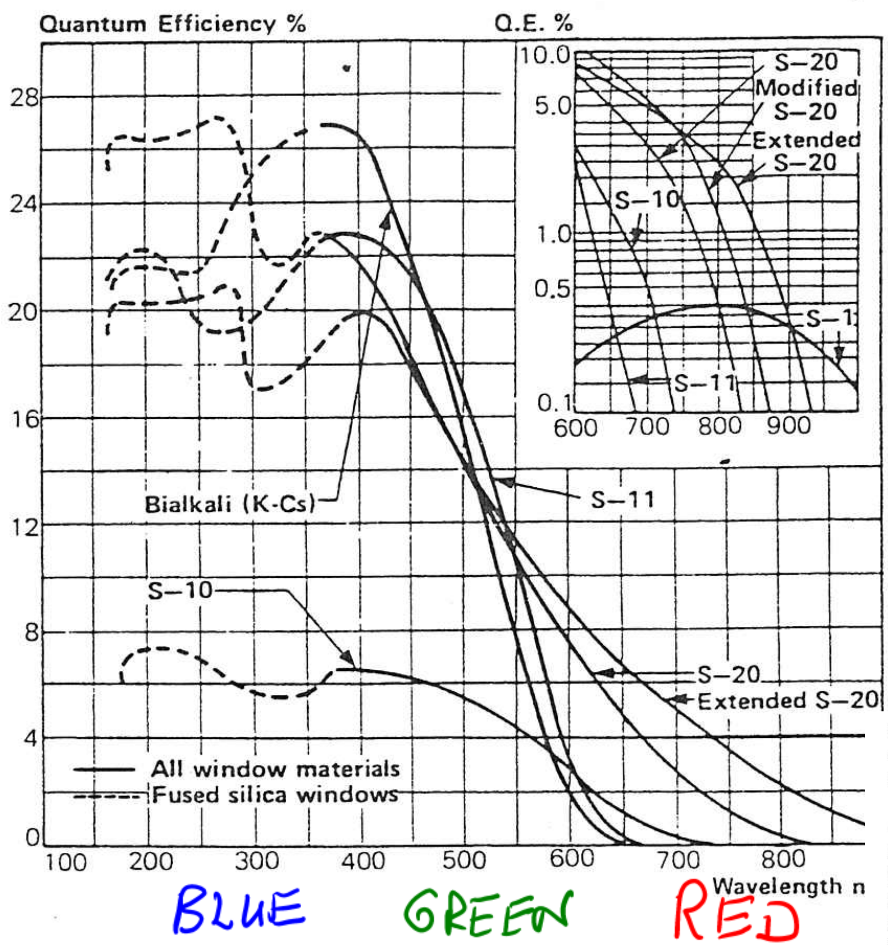

Table 8.1. Photocathode characteristics (from RTC catalog [8.3])

Cathode type	Composition	λ at peak response [nm]	Quantum efficiency at peak
S1 (C)	Ag – O – Cs	800	0.36
S4	SbCs	400	16
S11 (A)	SbCs	440	17
Super A	SbCs	440	22
S13 (U)	SbCs	440	17
S20 (T)	SbNa – KCs	420	20
S20R	SbNa – KCs	550	8
TU	SbNa – KCs	420	20
Bialkali	SbRb – Cs	420	26
Bialkali D	Sb – K – Cs	400	26
Bialkali DU	Sb – K – Cs	400	26
SB	Cs – Te	235	10

Modern Photodetectors

- Micro-channel plates
- Multi-anode pm
- Hybrid pm
- Visible light photon counters

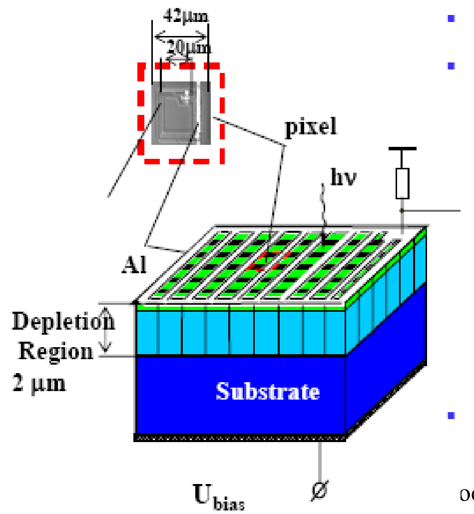

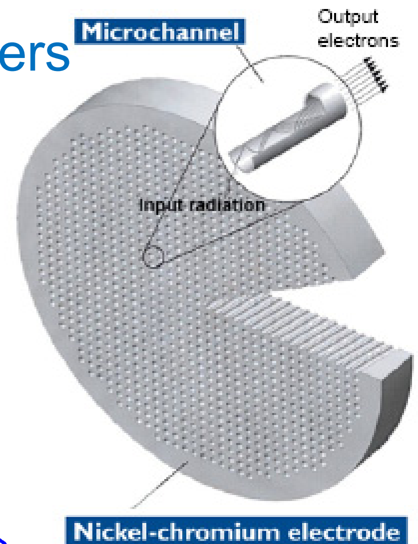

Multi Anode PM
example: Hamamatsu R5900 series.

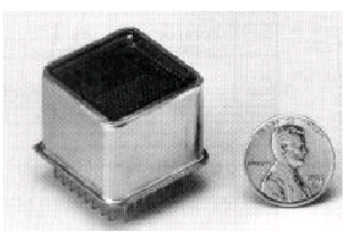

Up to 8x8 channels.
Size: 28x28 mm^2.
Active area 18x18 mm^2 (41%).
Bialkali PC: Q.E. = 20% at λ_{max} = 400 nm. Gain ≈ 10^6.

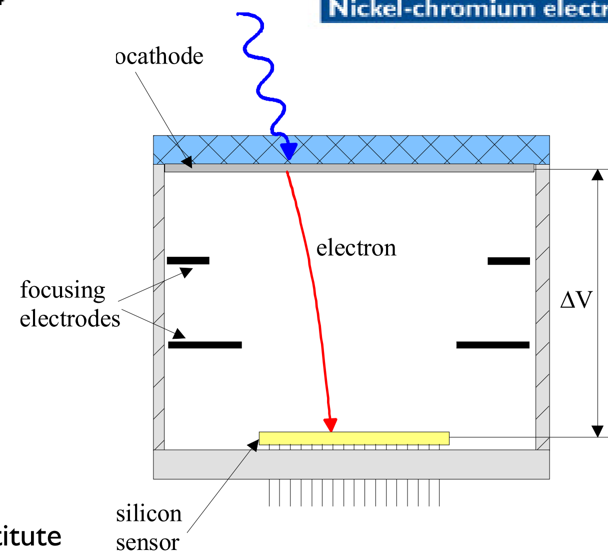

Schematic structure of MCP

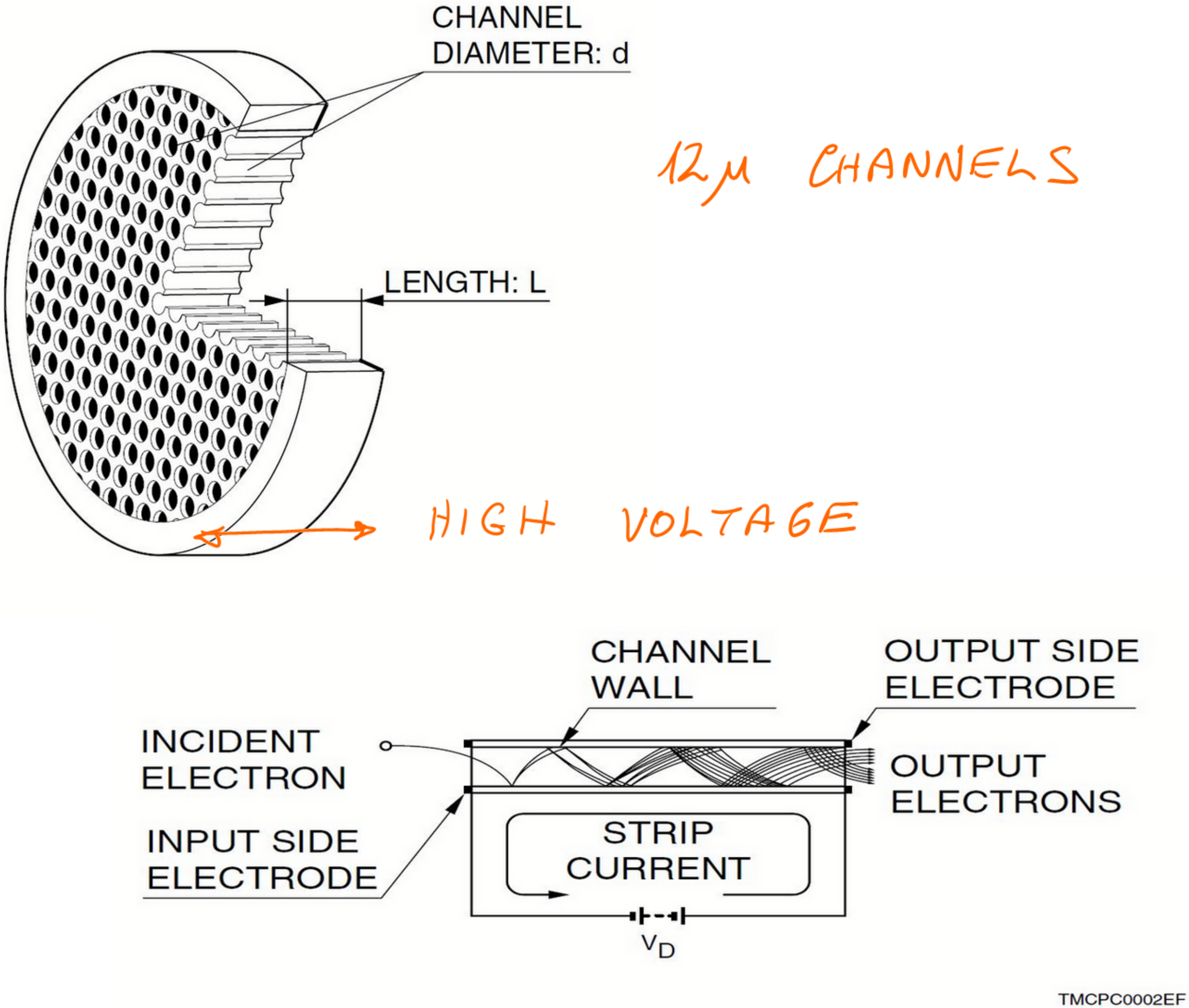

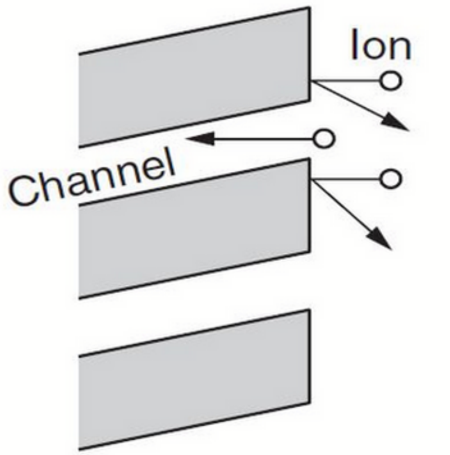

Cross-sectional view

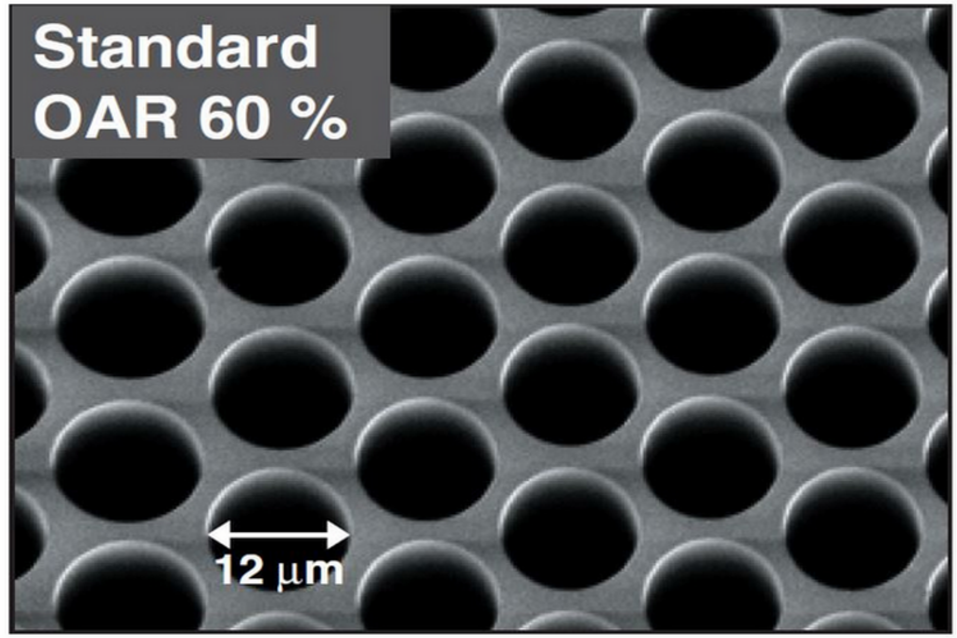

▲Shape of channel entrance (SEM image)

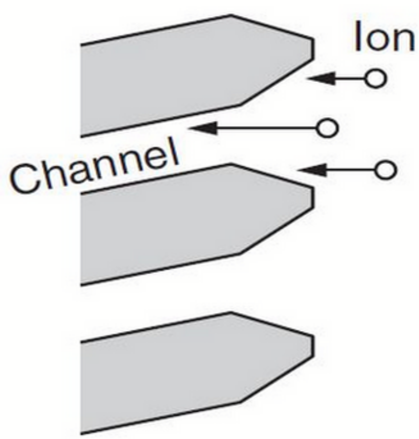

Cross-sectional view

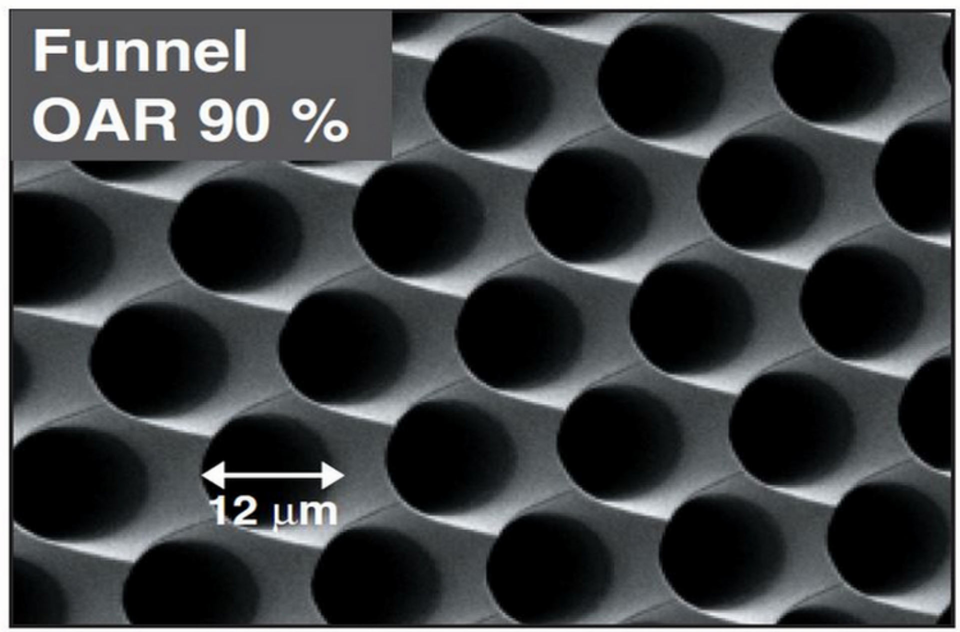

▲Shape of channel entrance (SEM image)

■MCP gain characteristics

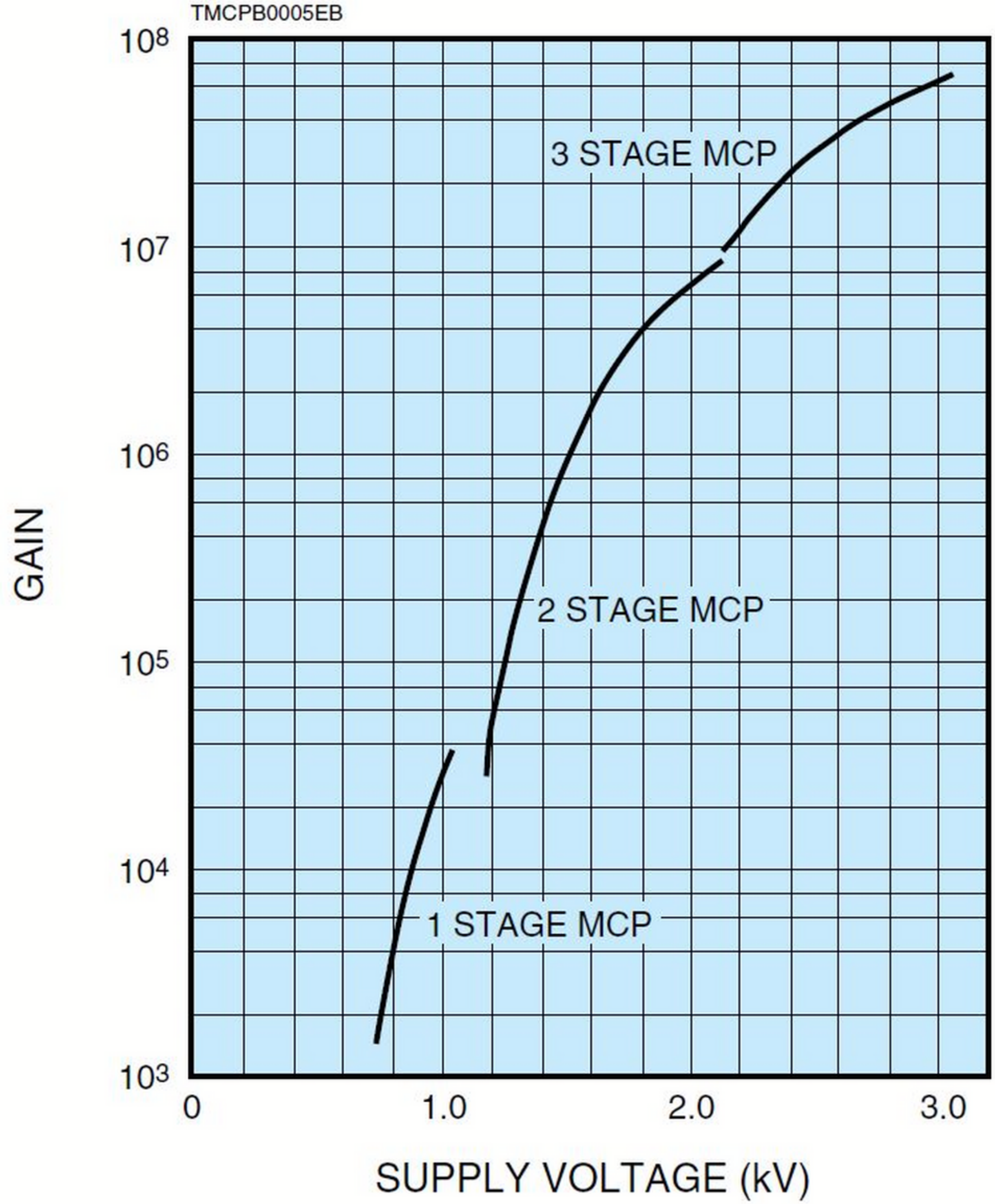

Principles of PIN Photodiodes

- As a photon flux Φ penetrates into a semiconductor, it will be absorbed as it progresses through the material.
- If $\alpha_s(\lambda)$ is the photon absorption coefficient at a wavelength λ, the *power level at a distance x into the material* is

$$P(x) = P_{in} \exp(-\alpha_s x)$$

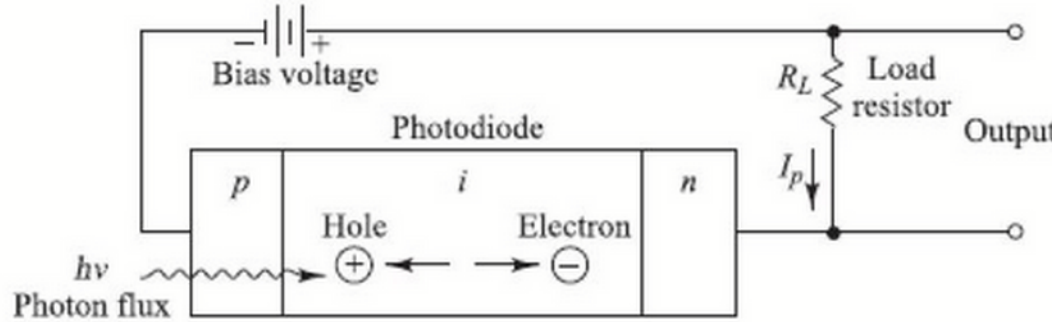

Absorbed photons trigger *photocurrent* I_p in the external circuitry

Photocurrent ∝ Incident Light Power

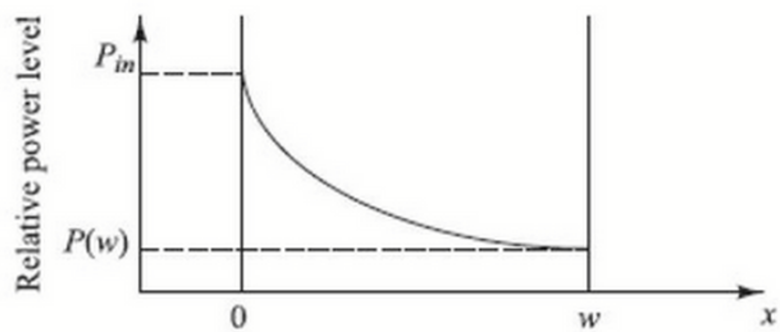

PIN Energy-Band Biagram

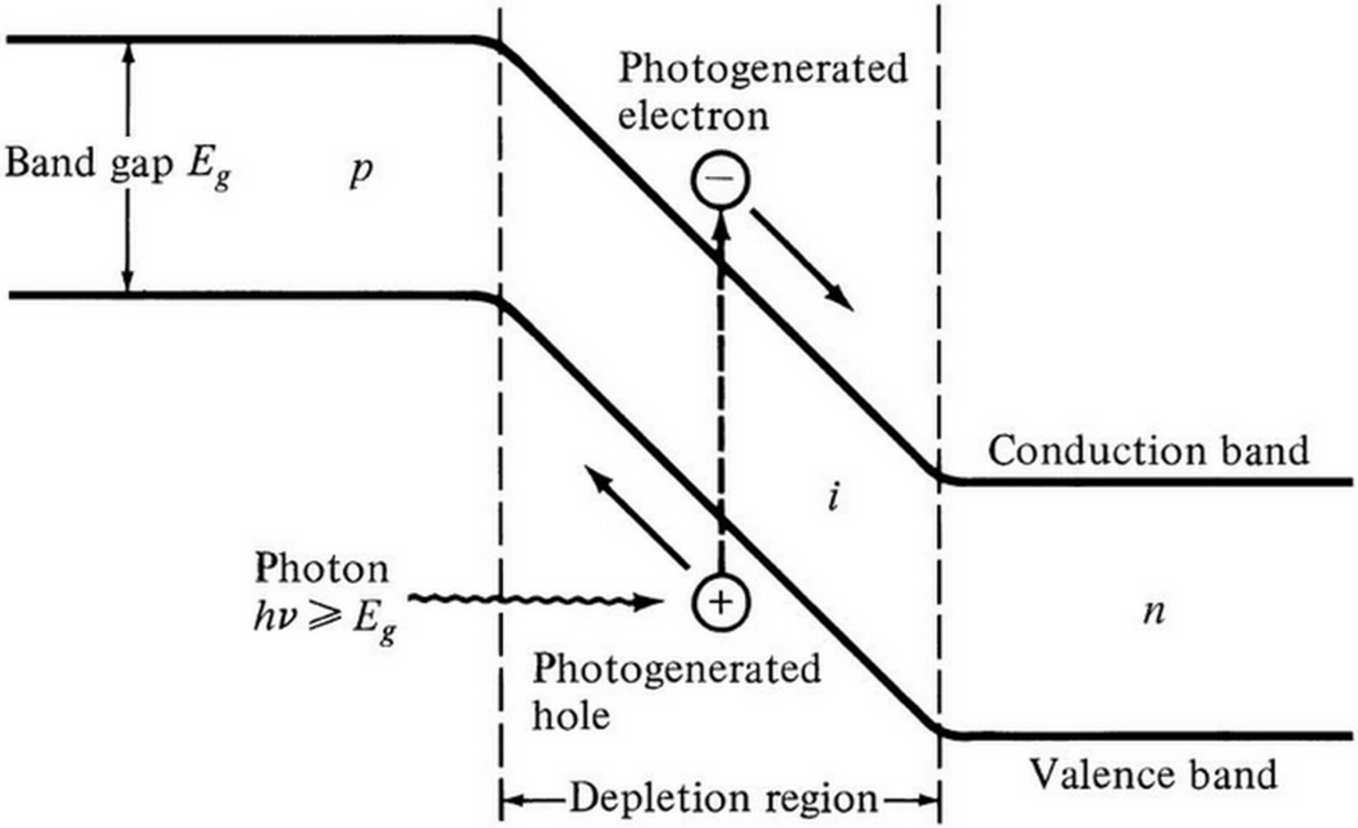

$$\lambda_c = \frac{hc}{E_g} = \frac{1.24}{E_g(eV)}\ \mu\text{m}$$

Cut off wavelength depends on the band gap energy

Avalanche Photodiode (APD)

- APD has an internal gain obtained by having a *high electric field* that energizes photo-generated electrons and holes
- These electrons and holes ionize bound electrons in the valence band upon colliding with them
- This mechanism is known as *impact ionization*
- The newly generated electrons and holes are also accelerated by the high electric field and they gain enough energy to cause further impact ionization
- This phenomena is called the avalanche effect.

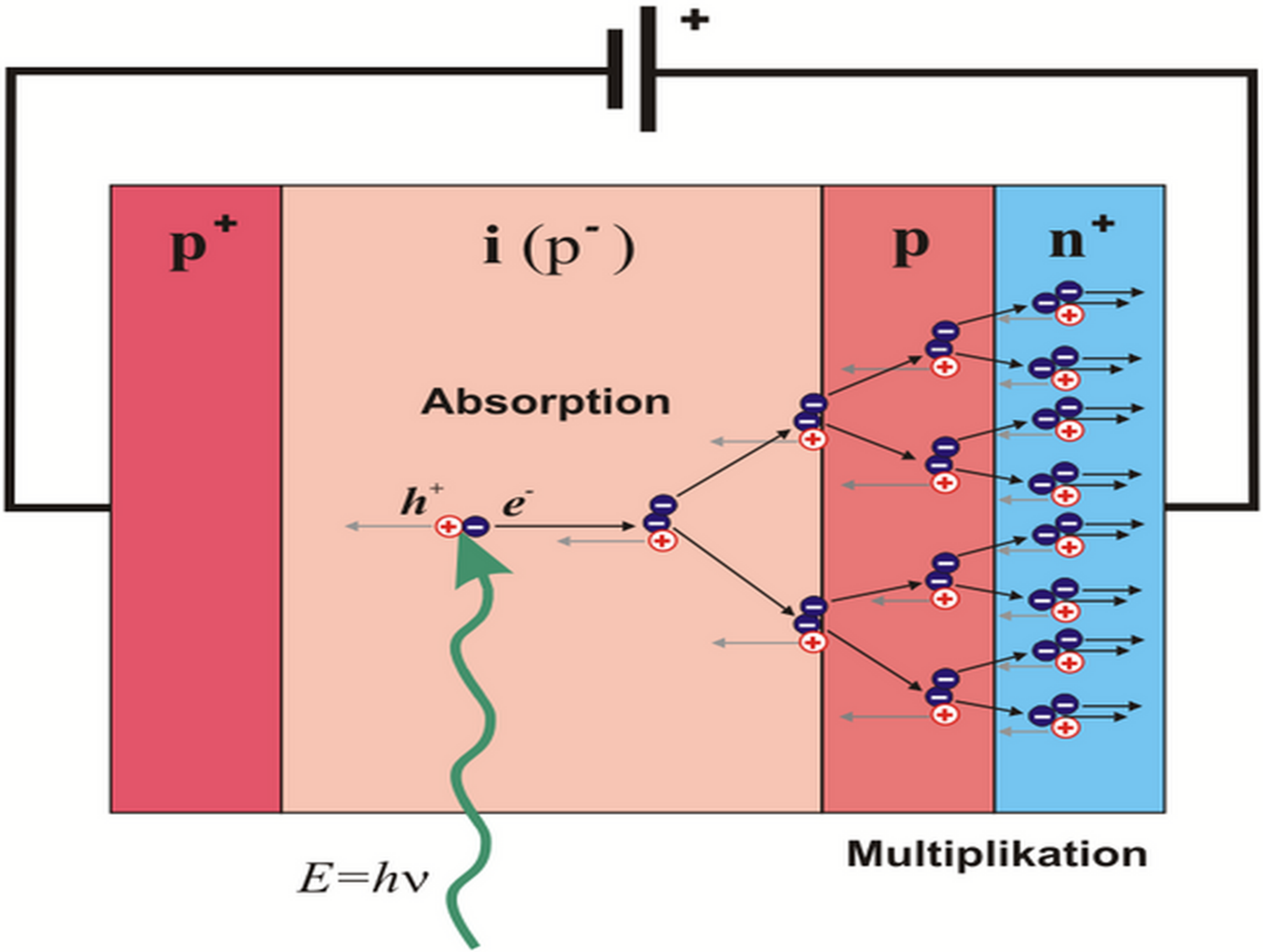

+
p+
i (p-)
p
n+
Absorption
h+
e-
E=hν
Multiplikation

VISIBLE LIGHT PHOTON COUNTER

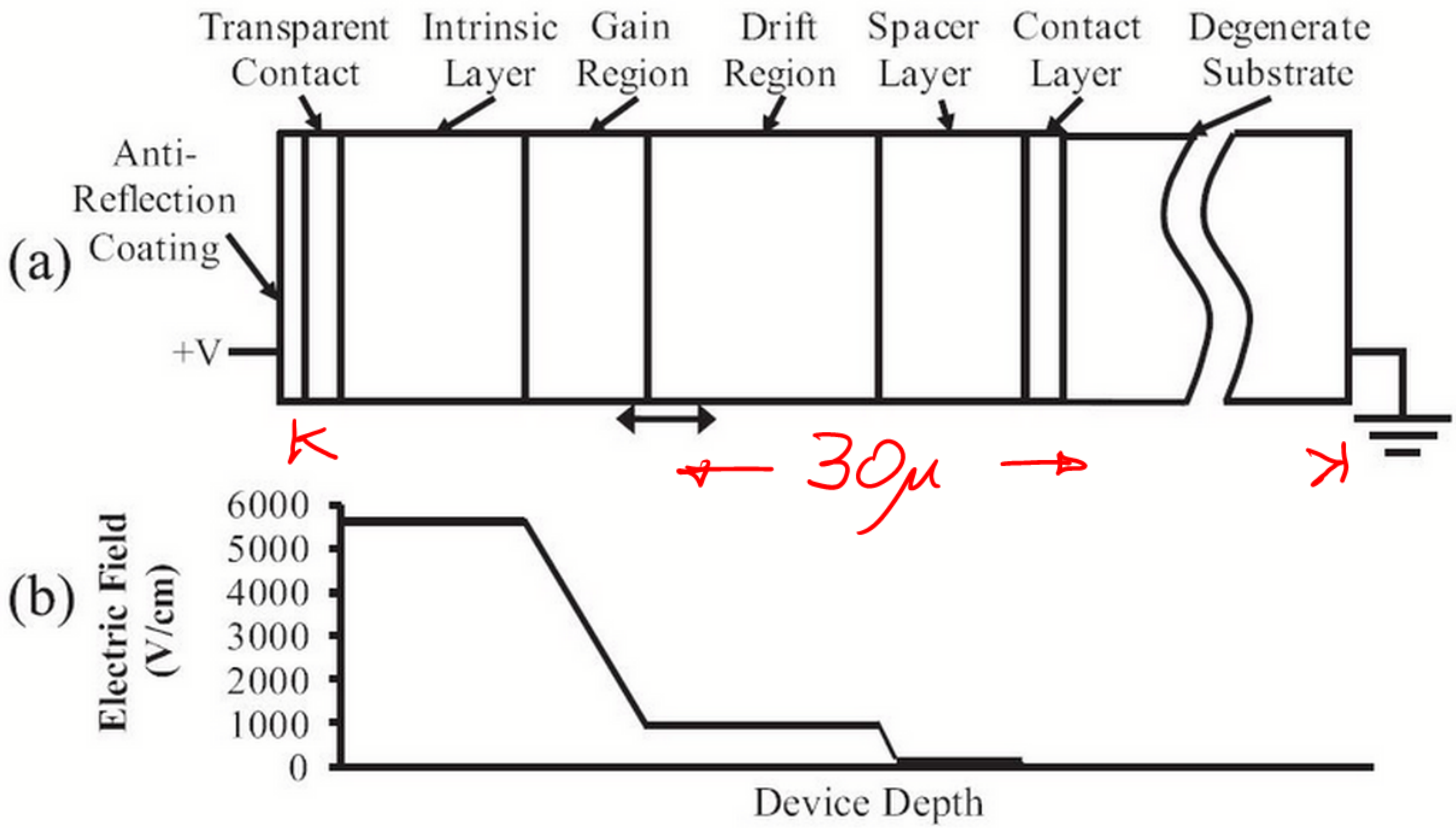

FIGURE 2.2: Schematic of the VLPC's (a) structure and (b) electric field profile. Total layer thickness of the epitaxial layers is $\sim 30\ \mu$ms.

CAN DETECT SINGLE PHOTONS

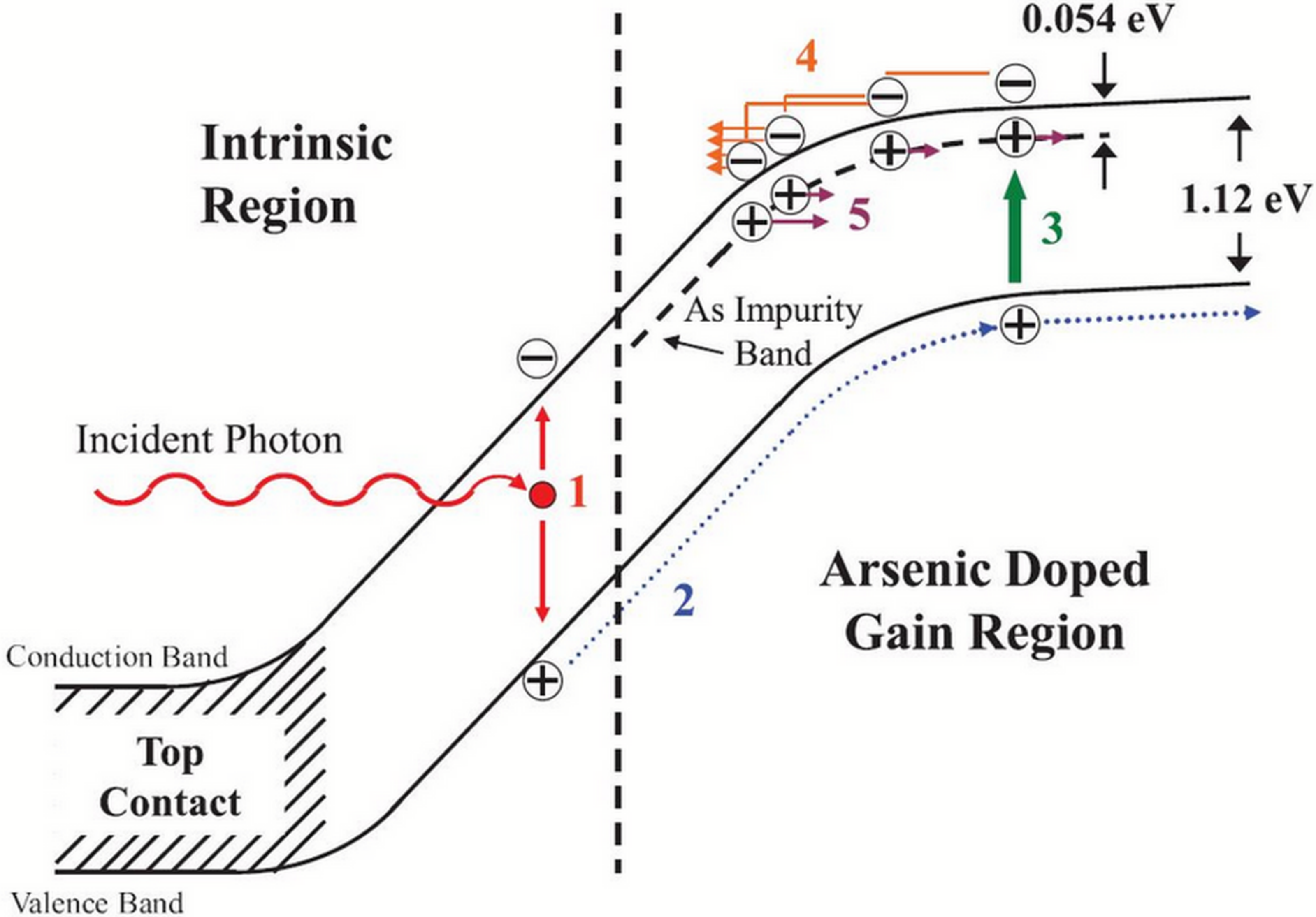

FIGURE 2.3: VLPC device operation. 1. An incident photon is absorbed generating an electron-hole pair. 2. The field in the device causes the hole to drift into the gain region. 3. The hole triggers an impact ionization event near the end of the gain region or within the drift region, which knocks an impurity electron into the conduction band. 4. The electron accelerates toward the front contact causing additional impact ionization events and starting an avalanche. 5. As the avalanche grows, D+ charges accumulate, which are slowly conducted away.

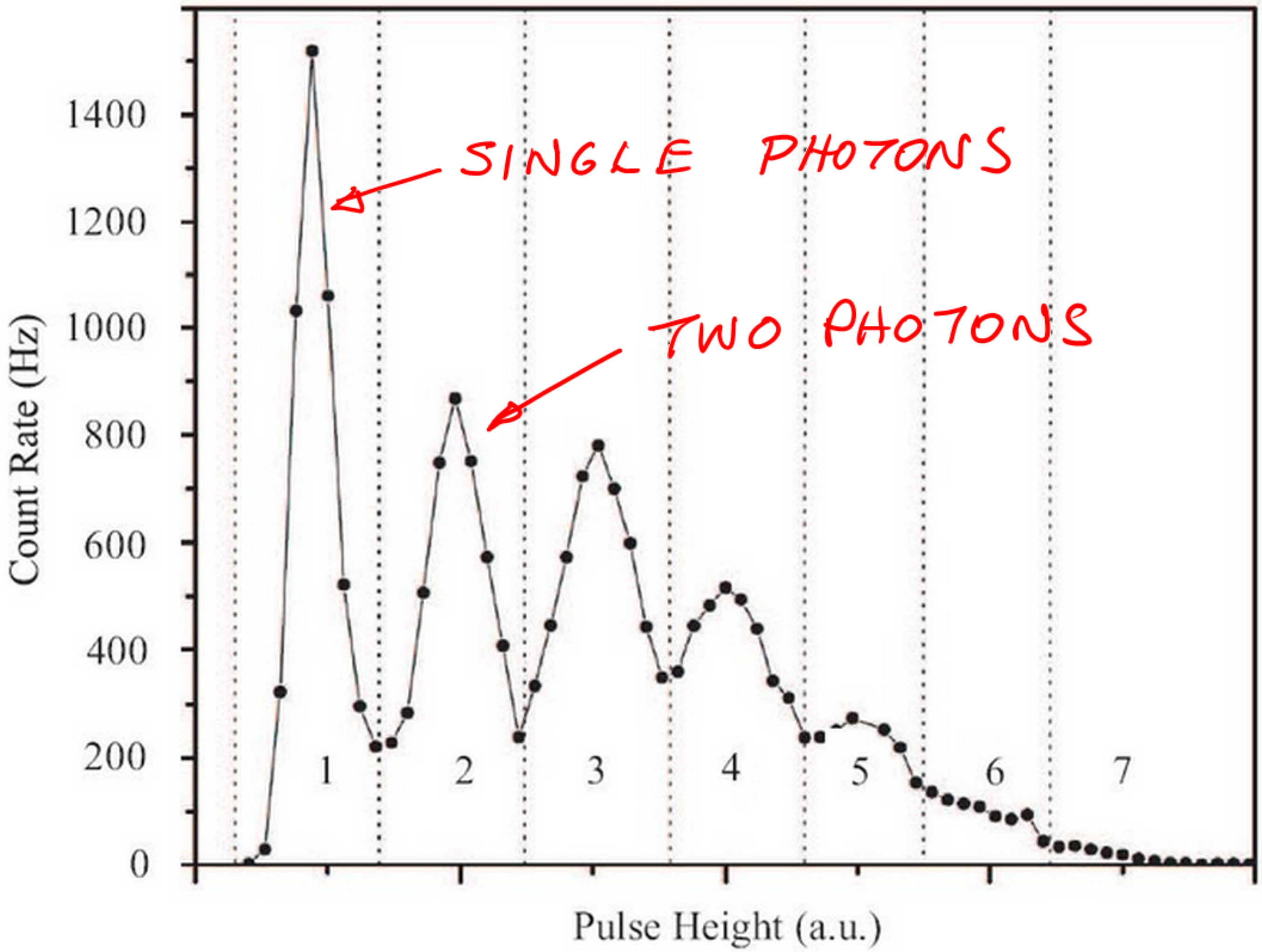

FIGURE 2.4: Pulse height distribution for the VLPC showing the size of the pulse depending on the number of photons detected. Dashed lines represent the voltage values at which thresholds would be set to determine photon number. Image reproduced with permission from [74].

Hybrid Photon Detectors (HPD)

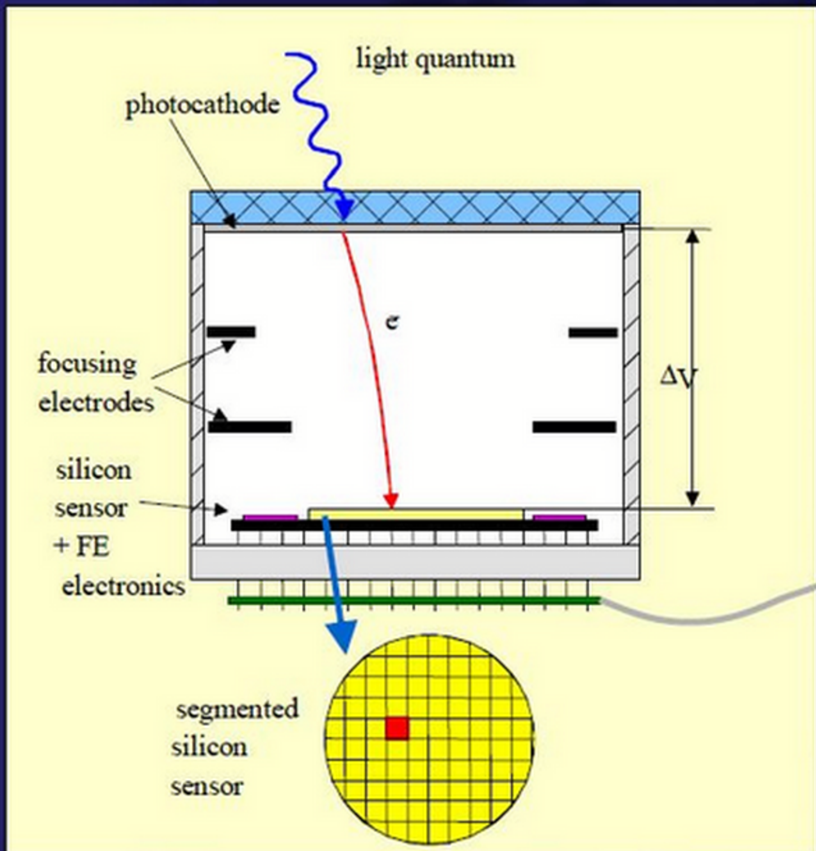

Combination of sensitivity of PMT with excellent spatial and energy resolution of silicon sensor

Gain: $$G \approx \frac{e \cdot U_C}{3.6\,\text{eV}}$$ U_C = 20 kV → G ~ 5000

Gain is achieved in a single dissipative step !

$$\sigma_G \approx \sqrt{F \cdot G}$$ small compared to $\sigma_{electronics}$

Main advantages of HPD technology

- Excellent signal definition
- Allows for photon counting
- Free choice of segmentation (50 µm - 10 mm)
- Uniform sensitivity and gain
- no dead zones between pixels

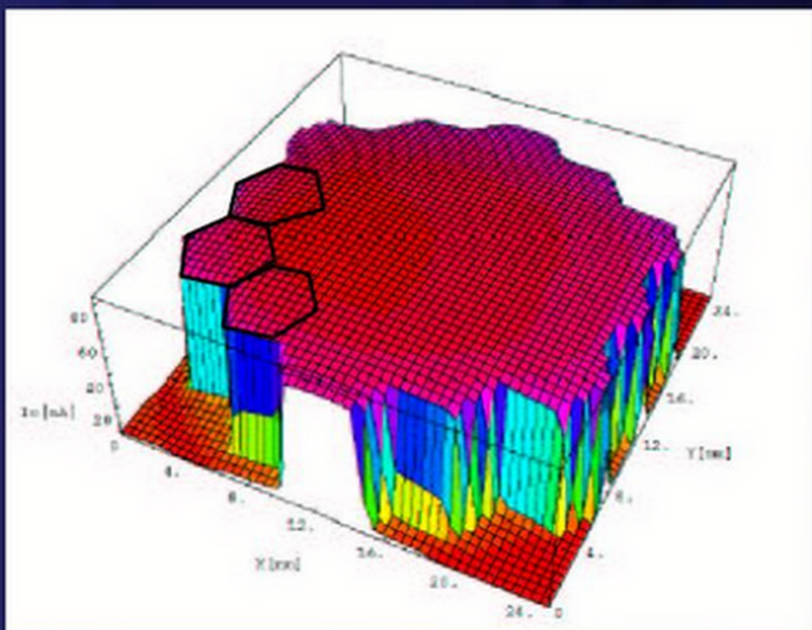

CMS HCAL
19-pixel HPD
(DEP, NL)

10-inch TOM HPD (U_C = -25 kV)

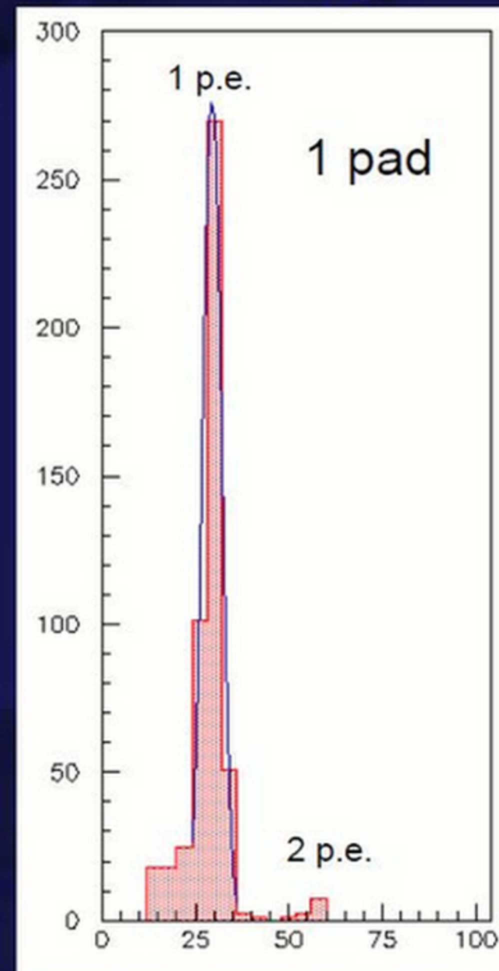

pulse height (ADC counts)

Drawbacks

- Rel. low gain (3000 - 8000) → low noise electronics required
- Expressed sensitivity to magnetic fields

The 5-inch Pad HPD
(originally developed for LHCb RICH)

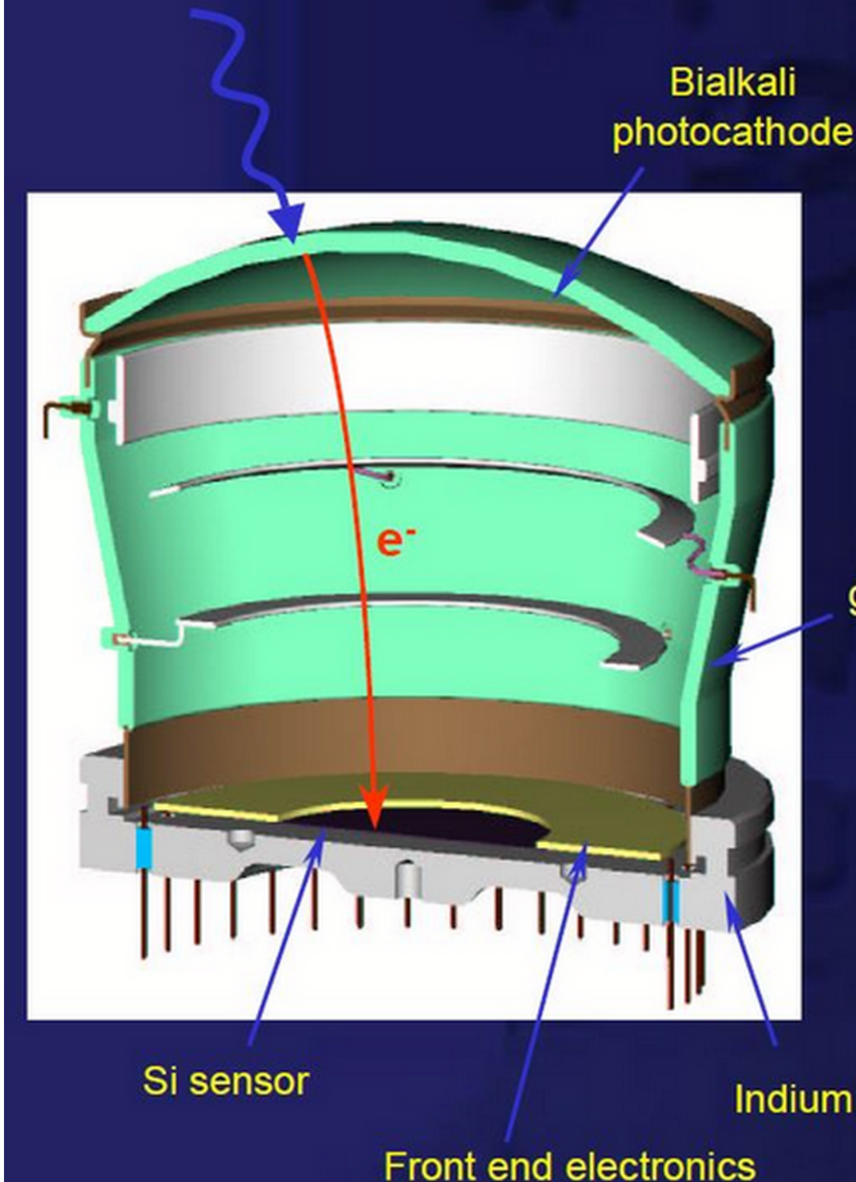

electron optics

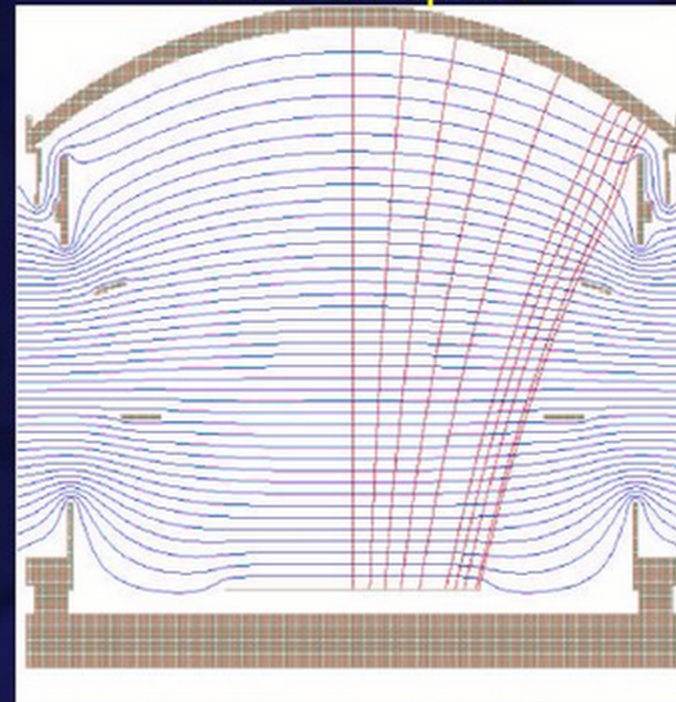

Si sensor and electronics

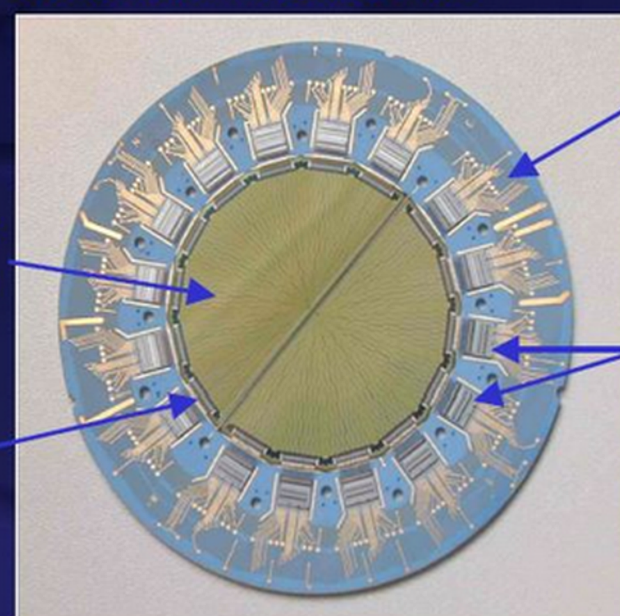

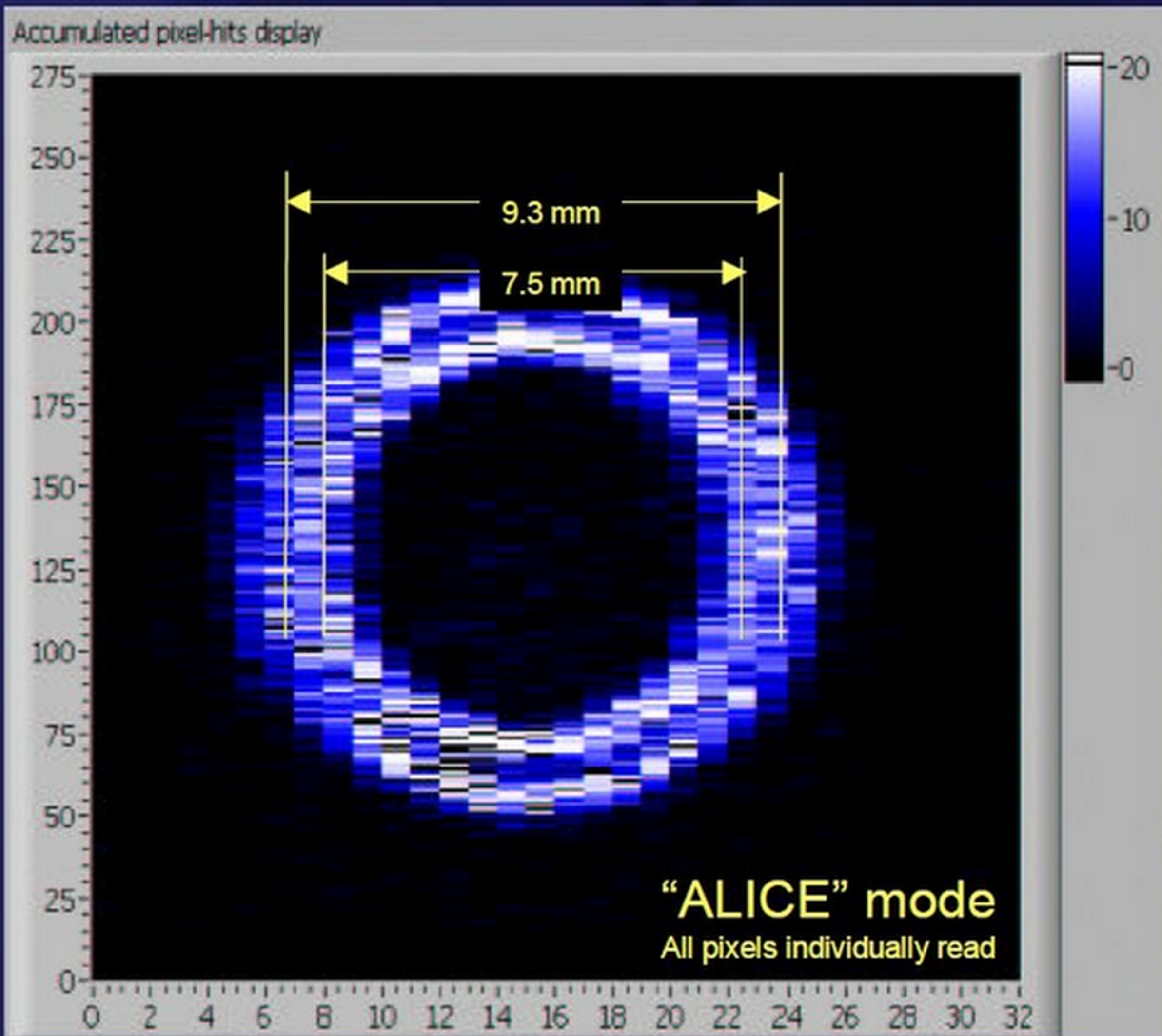

Online event display:

PS T9 - air radiator - 10 GeV/c

Double rings of e^- and π^-

First performance estimates meet all specifications, except det. efficiency ε_{det} ~ 0.87 (prel.)

Multi Anode Photo Multiplier Tubes

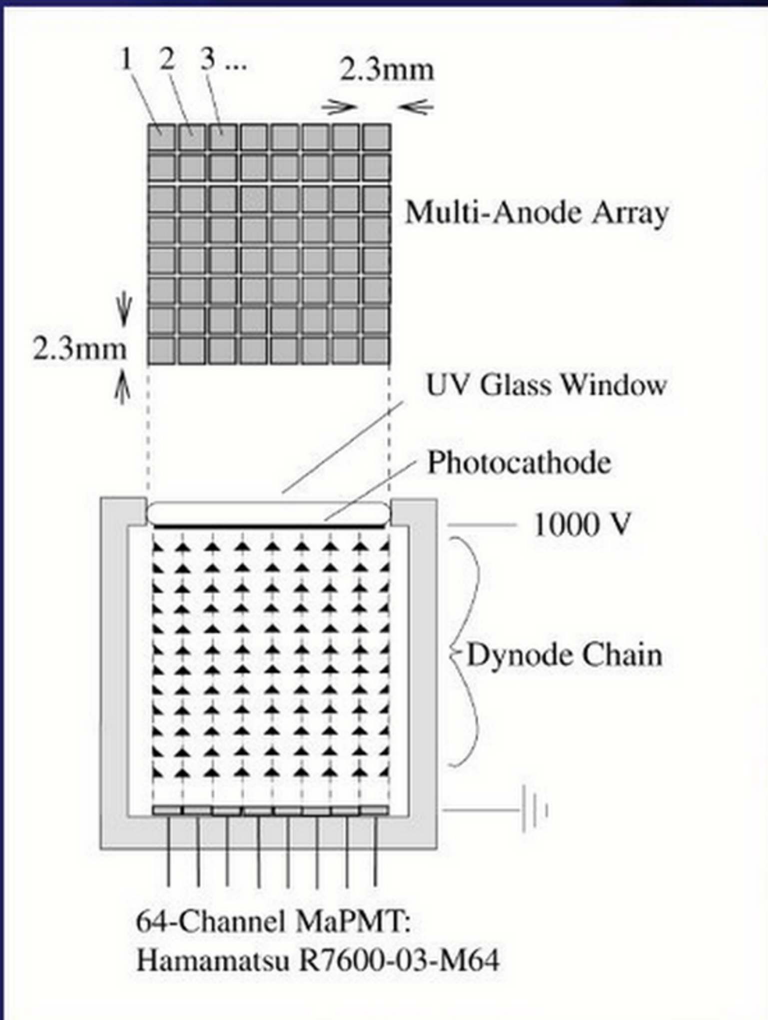

Principle

- Stacks of micro machined perforated metal sheets act as independent dynode channels.
- Independent anodes receive avalanches.

Issues

- Active area coverage
- Gain uniformity
- Cross talk
- Sensitivity to magnetic fields

Limitations

- Number of independent channels (~100)
- Pixel size (~mm)

What is the real active area ?

Principle of metal channel dynodes

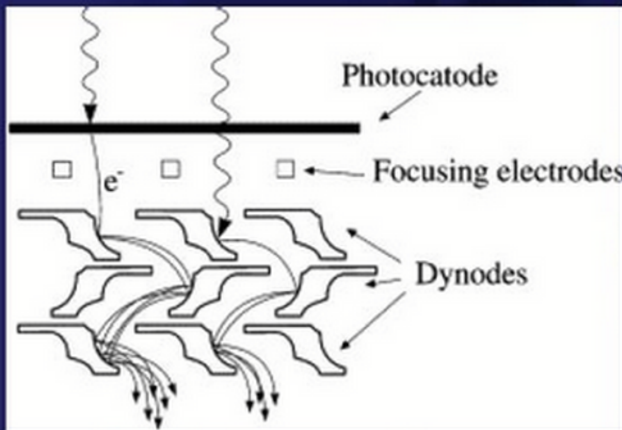

Example: Hamamatsu R7600-M64
64 cells of 2.3 mm □

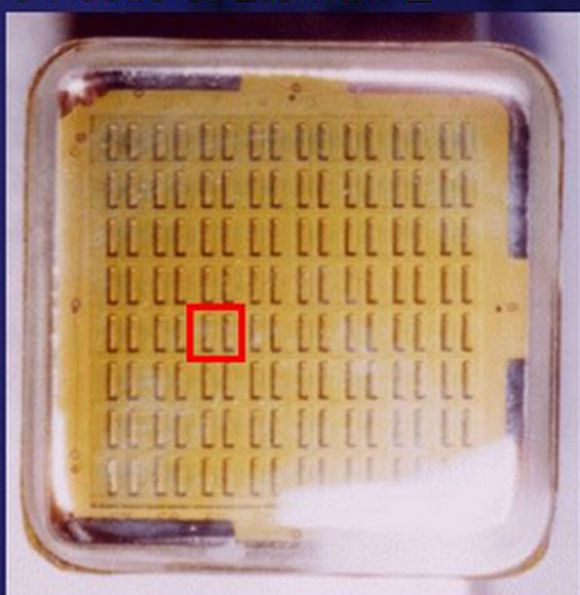

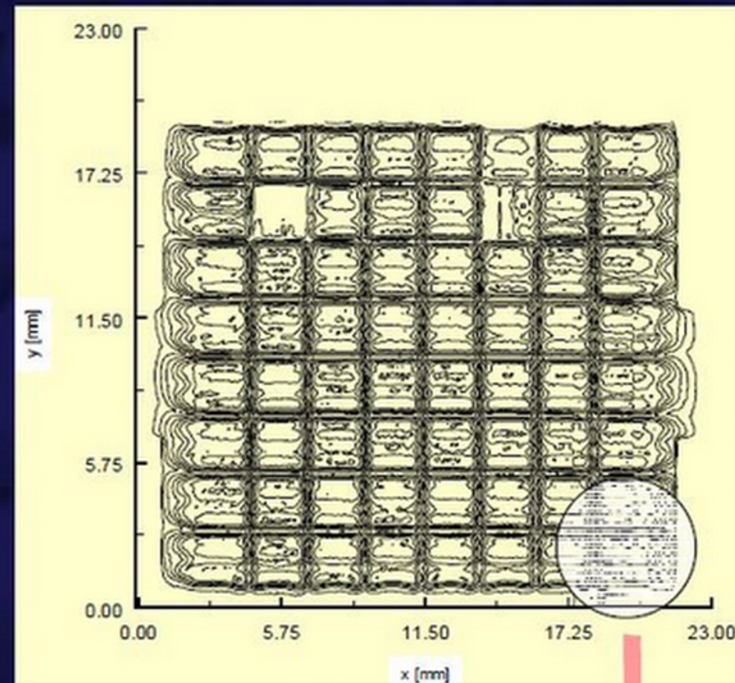

A. Duane et al. LHCb 98-039

There are gaps between cells !